ALEX(01)-TR-76-01

PRELIMINARY EVALUATION OF THE IRANIAN LONG PERIOD ARRAY

TECHNICAL REPORT NO. 1

VELA NETWORK EVALUATION AND AUTOMATIC PROCESSING RESEARCH

Prepared by
Alan C. Strauss

TEXAS INSTRUMENTS INCORPORATED
Equipment Group
Post Office Box 6015
Dallas, Texas 75222

Prepared for

AIR FORCE TECHNICAL APPLICATIONS CENTER
Alexandria, Virginia 22314

Sponsored by

ADVANCED RESEARCH PROJECTS AGENCY
Nuclear Monitoring Research Office
ARPA Program Code No. 6F10
ARPA Order No. 2551

29 October 1976

Acknowledgment: This research was supported by the Advanced Research Projects Agency, Nuclear Monitoring Research Office, under Project VELA-UNIFORM, and accomplished under the technical direction of the Air Force Technical Applications Center under Contract Numb.r F08606-76-C-0011.

PRELIMINARY EVALUATION OF THE IRANIAN LONG PERIOD ARRAY

TECHNICAL REPORT NO. 1

VELA NETWORK EVALUATION AND AUTOMATIC PROCESSING RESEARCH

Prepared by
Alan C. Strauss

TEXAS INSTRUMENTS INCORPORATED
Equipment Group
Post Office Box 6015
Dallas, Texas 75222

Prepared for

AIR FORCE TECHNICAL APPLICATIONS CENTER
Alexandria, Virginia 22314

Sponsored by

ADVANCED RESEARCH PROJECTS AGENCY
Nuclear Monitoring Research Office
ARPA Program Code No. 6F10
ARPA Order No. 2551

29 October 1976

Acknowledgment: This research was supported by the Advanced Research Projects Agency, Nuclear Monitoring Research Office, under Project VELA-UNIFORM, and accomplished under the technical direction of the Air Force Technical Applications Center under Contract Number F08606-76-C-0011.

UNCLASSIFIED

SECURITY CLASSIFICATION OF THIS PAGE (When Data Entered)

REPORT DOCUMENTATION PAGE

READ INSTRUCTIONS BEFORE COMPLETING FORM

1. REPORT NUMBER
2. GOVT ACCESSION NO.
3. RECIPIENT'S CATALOG NUMBER

4. TITLE (and Subtitle)
PRELIMINARY EVALUATION OF THE IRANIAN LONG PERIOD ARRAY.

5. TYPE OF REPORT & PERIOD COVERED
Technical Rept.

6. PERFORMING ORG. REPORT NUMBER
ALEX(01)-TR-76-01

7. AUTHOR(s)
Alan C. Strauss

8. CONTRACT OR GRANT NUMBER(s)
F08606-76-C-0011
ARPA Order-2515

9. PERFORMING ORGANIZATION NAME AND ADDRESS
Texas Instruments Incorporated
Equipment Group
Dallas, Texas 75222

10. PROGRAM ELEMENT, PROJECT, TASK AREA & WORK UNIT NUMBERS
VELA T/6705/B/ETR

11. CONTROLLING OFFICE NAME AND ADDRESS
Advanced Research Projects Agency
Nuclear Monitoring Research Office
Arlington, Virginia 22209

12. REPORT DATE
29 October 1976

13. NUMBER OF PAGES
74

14. MONITORING AGENCY NAME & ADDRESS (if different from Controlling Office)
Air Force Technical Applications Center
VELA Seismological Center
Alexandria, Virginia 22314

15. SECURITY CLASS. (of this report)
UNCLASSIFIED

15a. DECLASSIFICATION/DOWNGRADING SCHEDULE

16. DISTRIBUTION STATEMENT (of this Report)

77p.

APPROVED FOR PUBLIC RELEASE, DISTRIBUTION UNLIMITED

17. DISTRIBUTION STATEMENT (of the abstract entered in Block 20, if different from Report)

18. SUPPLEMENTARY NOTES

ARPA Order No. 2551

19. KEY WORDS (Continue on reverse side if necessary and identify by block number)

Seismology	Data Quality
Remote Site	Beamforming Gains
Central Recording Station	Detection Capability
Station Processor	M_s-m_b Relationships

20. ABSTRACT (Continue on reverse side if necessary and identify by block number)

This report describes the preliminary evaluation of the Iranian Long Period Array (ILPA). This evaluation was performed by Texas Instruments Incorporated at the Seismic Data Analysis Center in Alexandria, Virginia.

The major areas of study in this evaluation are:

- Evaluation of the data quality and sources of data errors,

DD FORM 1 JAN 73 1473 EDITION OF 1 NOV 65 IS OBSOLETE

UNCLASSIFIED

SECURITY CLASSIFICATION OF THIS PAGE (When Data Entered)

405076

20. continued

- Estimation of beamforming gains,
- Estimation of seismic event detection thresholds,
- Determination of seismic event M_S-m_b relationships.

Conclusions regarding the above points and plans for future work are also presented.

ABSTRACT

This report describes the preliminary evaluation of the Iranian Long Period Array (ILPA). This evaluation was performed by Texas Instruments Incorporated at the Seismic Data Analysis Center in Alexandria, Virginia.

The major areas of study in this evaluation are:

- Evaluation of the data quality and sources of data errors
- Estimation of beamforming gains
- Estimation of seismic event detection thresholds
- Determination of seismic event M_s-m_b relationships.

Conclusions regarding the above points and plans for future work are also presented.

TABLE OF CONTENTS

SECTION	TITLE	PAGE
	ABSTRACT	iii
I.	INTRODUCTION	I-1
II.	IRANIAN LONG-PERIOD ARRAY SYSTEM DESIGN	II-1
	A. DESCRIPTION OF THE ARRAY	II-1
	B. THE DATA RECORDING FORMAT	II-5
III.	DATA BASE AND METHOD OF ANALYSIS	III-1
	A. DATA BASE	III-1
	B. METHOD OF DATA PROCESSING AND ANALYSIS	III-3
IV.	DATA QUALITY	IV-1
	A. DATA TAPE ERRORS	IV-1
	B. NUMBER OF GOOD SITES	IV-5
	C. SUMMARY OF OBSERVATIONS ON DATA QUALITY	IV-6
V.	SIGNAL ANALYSIS	V-1
	A. SIGNAL-TO-NOISE RATIO GAINS DUE TO BEAMFORMING	V-1
	B. SHORT-PERIOD ILPA DETECTION CAPABILITY	V-4
	C. INDIRECT ESTIMATES OF LONG-PERIOD DETECTION CAPABILITY	V-7
	D. DIRECT ESTIMATES OF LONG-PERIOD DETECTION CAPABILITY	V-8
	E. M_s-m_b RELATIONSHIPS AT ILPA	V-22

TABLE OF CONTENTS
(continued)

SECTION	TITLE	PAGE
VI.	CONCLUSIONS	VI-1
VII.	REFERENCES	VII-1
	APPENDIX A	A-1

LIST OF FIGURES

FIGURE	TITLE	PAGE
II-1	ILPA SITE LOCATIONS	II-3
II-2	SATELLITE TAPE FORMAT	II-6
III-1	NUMBER OF EVENTS AS A FUNCTION OF EPICENTRAL DISTANCE	III-2
III-2	DATA PROCESSING METHOD	III-5
IV-1	THE DATA-SHIFT ERROR	IV-2
V-1	ILPA SHORT-PERIOD DETECTION STATISTICS	V-6
V-2	ILPA LONG-PERIOD VERTICAL COMPONENT DETECTION STATISTICS: MIXED EVENTS, EVENTS CONTAINING MALFUNCTIONS, AND EVENTS FOR WHICH NO DATA WAS RECORDED TREATED AS NON-DETECTIONS	V-11
V-3	ILPA LONG-PERIOD TRANSVERSE COMPONENT DETECTION STATISTICS: MIXED EVENTS, EVENTS CONTAINING MALFUNCTIONS, AND EVENTS FOR WHICH NO DATA WAS RECORDED TREATED AS NON-DETECTIONS	V-12
V-4	ILPA LONG-PERIOD RADIAL COMPONENT DETECTION STATISTICS: MIXED EVENTS, EVENTS CONTAINING MALFUNCTIONS, AND EVENTS FOR WHICH NO DATA WAS RECORDED TREATED AS NON-DETECTIONS	V-13
V-5	ILPA REFERENCE SITE VERTICAL COMPONENT DETECTION STATISTICS	V-14
V-6	ILPA BEAM VERTICAL COMPONENT DETECTION STATISTICS	V-15
V-7	ILPA BEAM VERTICAL COMPONENT DETECTION STATISTICS $0^{\circ} \leq \Delta < 20^{\circ}$	V-18
V-8	ILPA BEAM VERTICAL COMPONENT DETECTION STATISTICS $20^{\circ} \leq \Delta < 50^{\circ}$	V-19

LIST OF FIGURES
(continued)

FIGURE	TITLE	PAGE
V-9	ILPA BEAM VERTICAL COMPONENT DETECTION STATISTICS $50^{\circ} \leq \Delta < 80^{\circ}$	V-20
V-10	ILPA BEAM DETECTION STATISTICS: DETECTION ON ONE COMPONENT REQUIRED TO DECLARE AN EVENT DETECTION	V-21
V-11	ILPA BEAM DETECTION STATISTICS: DETECTION ON ALL COMPONENTS REQUIRED TO DECLARE AN EVENT DETECTION	V-23
V-12	ILPA INSTRUMENT RESPONSE NORMALIZED AT 25 SECONDS	V-25
V-13	ILPA VERTICAL COMPONENT M_s-m_b RELATIONSHIP FOR 20 SECOND M_s	V-26
V-14	ILPA TRANSVERSE COMPONENT M_s-m_b RELATIONSHIP FOR 20 SECOND M_s	V-27
V-15	ILPA RADIAL COMPONENT M_s-m_b RELATIONSHIP FOR 20 SECOND M_s	V-28
V-16	M_s-m_b RELATIONSHIPS AT 20, 30, AND 40 SECONDS PERIOD	V-30

LIST OF TABLES

TABLE	TITLE	PAGE
II-1	REMOTE SITE COORDINATES	II-2
IV-1	SUMMARY OF PARITY AND TIMING ERRORS	IV-4
IV-2	SUMMARY OF SITE REJECTION STATISTICS	IV-7
V-1	SIGNAL-TO-NOISE RATIO GAINS DUE TO BEAMFORMING	V-3
V-2	RMS NOISE SUPPRESSION AND PEAK SIGNAL SUPPRESSION DUE TO BEAMFORMING	V-5
V-3	INDIRECT ESTIMATES OF LONG-PERIOD DETECTION CAPABILITY; VERTICAL COMPONENT	V-9
V-4	SUMMARY OF DETECTION CAPABILITY INFORMATION; 50 PERCENT BODYWAVE MAGNITUDE (m_b) DETECTION CAPABILITY	V-17
V-5	M_s-m_b FIT SLOPE AND INTERCEPT VALUES	V-29
A-1	EVENT PARAMETERS	A-2

SECTION I
INTRODUCTION

This report presents the results of a preliminary evaluation of the seven element Iranian Long-Period Array (ILPA). Since data did not begin to arrive until the end of May 1976, it was necessary to sharply curtail the goals of this evaluation. In the limited time remaining in the contract period, emphasis was placed on evaluating the quality of the ILPA data and obtaining estimates of ILPA detection capability. The specific areas of investigation include:

- Data quality
- Sources of data errors
- Beamforming gains
- Seismic event detection thresholds
- Seismic event M_s-m_b relationships.

A brief description of the Iranian Long Period Array is given in Section II. The data base and data processing methods are described in Section III. Data quality and sources of data errors are discussed in Section IV. Beamforming gains, detection thresholds, and M_s-m_b relationships are discussed in Section V. Finally, the results of this preliminary evaluation of the ILPA data are summarized in Section VI.

SECTION II

IRANIAN LONG-PERIOD ARRAY SYSTEM DESIGN

A. DESCRIPTION OF THE ARRAY

The Iranian Long Period Array is a seismic installation comprised of a central recording station and an array of seven remote sites. The locations of these sites are listed in Table II-1 and shown in Figure II-1.

Each remote site is composed of a three-component sensor subsystem, a data acquisition subsystem, a telemetry subsystem, and a power subsystem. The three-component seismometer of the sensor subsystem is located in a 100 meter borehole to reduce wind-generated noise. The seismometer, a signal conditioning unit, and a remote control unit make up the sensor subsystem. The data acquisition subsystem, housed in a small building near the borehole, contains a six-channel multiplexer, a sample-and-hold module, a binary gain-ranging amplifier, an analog-to-digital converter, and data formatting and control logic. The data acquisition subsystem converts signals from the sensor subsystem to the correct format for transmission to the central recording station.

The remote site telemetry subsystem transmits signals from the data acquisition subsystem to the central recording station and receives command signals from the central recording station. The equipment at each site consists of an antenna, a duplexer which permits transmitting and receiving with a single antenna, a transmitter, a receiver, transmit and receive modules, and remote control logic. One telemetry subsystem includes a relay station, located at site 5, which relays data between site 6 and the central recording station. This relay is necessary because site 6 does not have line-of-sight with the central recording station.

TABLE II-1

REMOTE SITE COORDINATES

Site	Location		Distance From Reference Site (km)	
	Latitude ($^{\circ}$N)	Longitude ($^{\circ}$E)	North	East
1 (ref)	35°24'58.3"	50°41'19.5"	0.0	0.0
2	35°39'46.1"	50°53'51.5"	27.277	19.035
3	35°28'34.0"	51°01'25.5"	6.217	30.377
4	35°14'19.3"	50°54'04.2"	-19.536	19.162
5	35°12'46.2"	50°34'52.0"	-22.415	-9.830
6	35°28'25.2"	50°25'32.2"	5.815	-23.775
7	35°42'10.1"	50°36'32.0"	31.700	-6.951

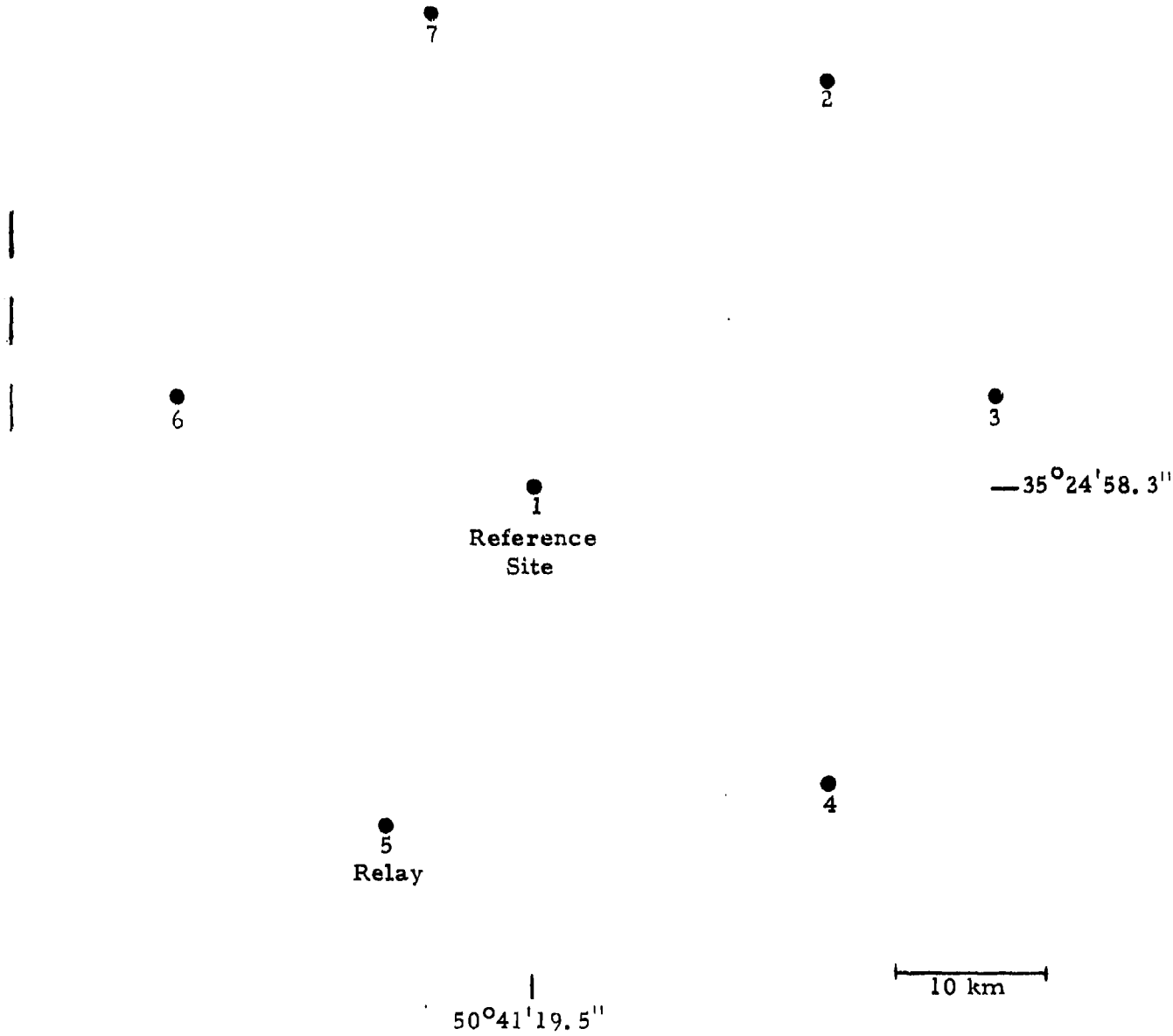

FIGURE II-1

ILPA SITE LOCATIONS

The central recording station processes and records data received from each site of the array. It contains the equipment necessary to transmit commands, receive and process data from the remote sites, and record the results of this processing on visual and magnetic recorders. A timing subsystem for synchronization of operations at the seven remote sites and the central recording station is also part of the central recording station. The equipment housed in the central recording station are the station processor, the visual recording subsystem, the magnetic digital tape recording subsystem, the timing subsystem, the telemetry subsystem, and the power subsystem.

The station processor contains the computing and control elements of the system, supplied by the central processing units. Each of the central processing units contains the same program and is capable of performing all on-line and off-line requirements of the system. The central processing unit which is manually placed on-line assumes the responsibility of performing on-line operations and transmits to the off-line central processing unit at one-second intervals. This transmission suppresses on-line operations by the off-line central processing unit. Failure to receive a transmission activates the on-line coding of the off-line central processing unit, switching the roles of the central processing units.

A teleprinter interfaces with each of the central processing units. These provide man-machine communications. Commands are given to the system by keyboard entry and the system status is printed out automatically.

The visual recording system converts the digital signals from the remote sites back to analog form for display on drum recorders and develocorders. The develocorders record the data on film, process the data, and store it. Viewing screens on the develocorders permit viewing of the film. A second visual display is made by the drum recorders on 30x90 centimeter recording paper.

The digital magnetic recording system records three-component long-period data from the remote sites. One recorder is reserved as backup in case of an on-line recording drive failure. This system is also used for the tasks of providing data for beamforming and display and editing data to another tape. It was intended that data would be transmitted to the United States by satellite relay. To accomplish this, the data is reformatted into the satellite format of Figure II-2. To date, the data is not relayed by satellite but is recorded on magnetic tape in this format at ILPA. The tapes are then shipped to the United States.

The telemetry system transmits command and control data to the remote sites as well as calibration signals to the sensor systems. This system also receives data from the remote sites via seven receivers. Each receiver drives a receiver module which interfaces through a separate I/O port to the central processing units. These interfaces perform serial-to-parallel conversion of incoming data and present each central processing unit with data on an interrupt basis.

The power system is designed to provide uninterrupted controlled power to the central processing station. When this system is completed, power from a motor generator will be automatically substituted via a transfer switch for commercial power during commercial power failures. The generator will be capable of sustaining power for eight hours without refueling. The transfer switch will allow for a delay of up to five minutes before the generator is started. During this delay, battery power will maintain the system. These batteries will power the system for one hour.

B. THE DATA RECORDING FORMAT

The primary output of the data recording system available to us is the digital magnetic tape. This tape is nine-track, recorded in the satellite tape format at 800 bits per inch, using two's complement binary arithmetic.

Satellite Tape Format

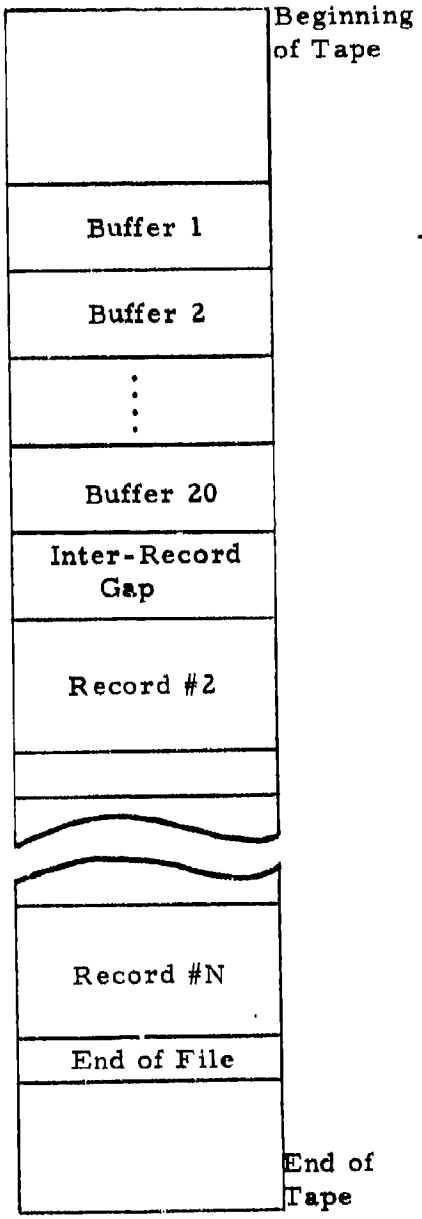

Format of Satellite Output Buffer*

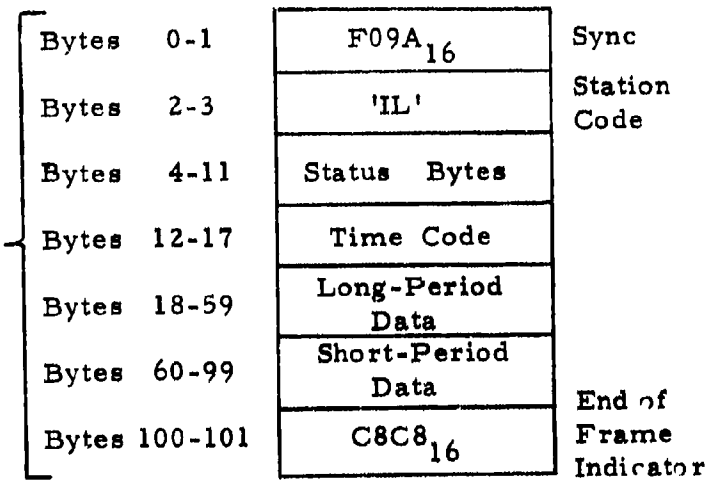

Each record of 20 buffers contains 20 seconds of data.

24 hours per tape
800 bpi
9 track tape
8.5" reels

* Literals are in EBCDIC.

FIGURE II-2

SATELLITE TAPE FORMAT
(PAGE 1 OF 3)

Format of Status Bytes

Byte 0	Status Bits Site 1
Byte 1	Status Bits Site 2
Byte 2	Status Bits Site 3
Byte 3	Status Bits Site 4
Byte 4	Status Bits Site 5
Byte 5	Status Bits Site 6
Byte 6	Status Bits Site 7
Byte 7	Reserved

Bit 0 Sync Error

Bit 1 Calibration in progress

Bit 2 Deleted from beamforming

Bit 3 Faulty or Missing Long-Period Data

Bit 4 Faulty or Missing Short-Period Data

Bit 5-7 Reserved

(The above bits are set to one if the condition exists or to zero if the condition does not exist.)

Format of the Time Code*

Bytes 0-1	OYYD
Bytes 2-3	DDHH
Bytes 4-5	MMSS

Year: $0 \leq YY \leq 99_{10}$

Julian Day: $1 \leq DDD \leq 365_{10}$ (on leap year, $1 \leq DDD \leq 366_{10}$)

Hour: $0 \leq HH \leq 23_{10}$

Minute: $0 \leq MM \leq 59_{10}$

Second: $0 \leq SS \leq 59_{10}$

* Contents are in packed BCD.

FIGURE II-2

SATELLITE TAPE FORMAT
(PAGE 2 OF 3)

Format of Long-Period Data

Bytes 0-1	Site 1, Vertical Component
Bytes 2-3	Site 1, N-S Component
Bytes 4-5	Site 1, E-W Component
Bytes 6-7	Site 2, Vertical Component
Bytes 8-9	Site 2, N-S Component
Bytes 10-11	Site 2, E-W Component
⋮	
Bytes 36-37	Site 7, Vertical Component
Bytes 38-39	Site 7, N-S Component
Bytes 40-41	Site 7, E-W Component

Each component is in gain-ranged format.

Format of Short-Period Data

Bytes 0-1	Channel Datum for Zeroth Short-Period Frame
Bytes 2-3	Channel Datum for First Short-Period Frame
⋮	
Bytes 38-39	Channel Datum for Nineteenth Short-Period Frame

Each datum is in gain-ranged format.

(Only one channel of short-period data can be placed in the above buffer at any one time.)

FIGURE II-2

SATELLITE TAPE FORMAT
(PAGE 3 OF 3)

The satellite tape format is shown in Figure II-2, which illustrates the encoding of seven sites of three-component long-period data and one site of vertical-component short-period data.

The ILPA data word format consists of two bytes containing eight bits each in the following format:

- Byte 1: The four most significant bits define the gain factor. The next bit is the sign bit. The last three bits are the three most significant bits of the mantissa.
- Byte 2: These eight bits are the eight least significant bits of the mantissa. The mantissa is encoded in two's complement binary arithmetic.

The voltage registered by a sensor may be calculated by the formula:

$$\text{Voltage} = \frac{\text{Mantissa} * 2^{-(\text{gain code})}}{7FF_{16}} * 10_{10} \text{ volts}.$$

The gain code varies from 0 to 4 for short-period data and from 0 to A_{16} for long-period data. The number 10_{10} is the full-scale input signal accepted by the analog-to-digital converter. Using the above formula, the smallest signal which may be resolved is:

$$\text{Long-Period: } V_{MIN} = \frac{1 * 2^{-A_{16}}}{7FF_{16}} * 10_{10} = 4.773 \text{ microvolts } (\mu v)$$

$$\text{Short-Period: } V_{MIN} = \frac{1 * 2^{-4_{16}}}{7FF_{16}} * 10_{10} = 0.305 \text{ millivolts (mv)}$$

Thus, for long-period data, one computer count equals 4.773 μv, while for short-period data, one computer count equals 0.305 mv.

The sensor filters are set for output as follows:

$$\text{Long-Period: } 0.1 \frac{\text{volts}}{\text{micron}} \text{ at 25 seconds period}$$

$$\text{Short-Period: } 5.0 \frac{\text{volts}}{\text{micron}} \text{ at 1 second period .}$$

Therefore, the smallest signal in millimicrons which may be resolved is:

$$\text{Long-Period: } SIG_{MIN} = \frac{4.773 * 10^{-6} \text{ volts}}{0.1 \text{ volts/micron}} * 10^{3} \text{ millimicrons/micron}$$

$$= 0.04773 \text{ millimicrons (m}\mu\text{)}$$

$$\text{Short-Period: } SIG_{MIN} = \frac{0.305 * 10^{-3} \text{ volts}}{5.0 \text{ volts/micron}} * 10^{3} \text{ millimicrons/micron}$$

$$= 0.061 \text{ millimicrons (m}\mu\text{) .}$$

From this we see that the data is quantized at one computer count per 0.04773 millimicrons (20.951 cc/mμ) for long-period data at 25 seconds period. The short-period data is quantized at one computer count per 0.061 millimicrons (16.393 cc/mμ) at one second period.

A more detailed description of the ILPA system can be found in the operation and maintenance manual for the ILPA seismic system.

SECTION III
DATA BASE AND METHOD OF ANALYSIS

A. DATA BASE

For our first look at the Iranian Long-Period Array data, we selected the data recorded during the month of May 1976 since this was the earliest data we received. All events listed in the Norwegian Seismic Array (NORSAR) event lists for May 1976 which had epicenters in or near the Eurasian landmass were selected for processing. No effort was made to eliminate events which, based on origin time and epicenter location, could be expected to arrive at ILPA in the same time gate ("mixed signals"). This gave us a total of 281 events with epicentral distances ranging from 0.6 to 74.0 degrees. Figure III-1 shows that this event population can be broken down into a near-field subset (0° to 20°), a near teleseismic subset (20° to 50°), and a far teleseismic subset.

We note that at the time the data base was formed, we had no depth information for these events. Thus, it is entirely possible that some of these events occurred at depths significantly greater than 33 km (normal depth). Our interest in the depth of occurrence lies in the fact that deep events have significantly lower surface-wave magnitudes (M_s) than do shallow events. Thus, a set of deep and shallow events will have a greater M_s variance than will a set of shallow events alone. No presumed explosions were known by us to have occurred during May; so we cannot discuss the question of earthquake-presumed explosion discrimination. The seismic parameters of the data base are listed in Appendix A.

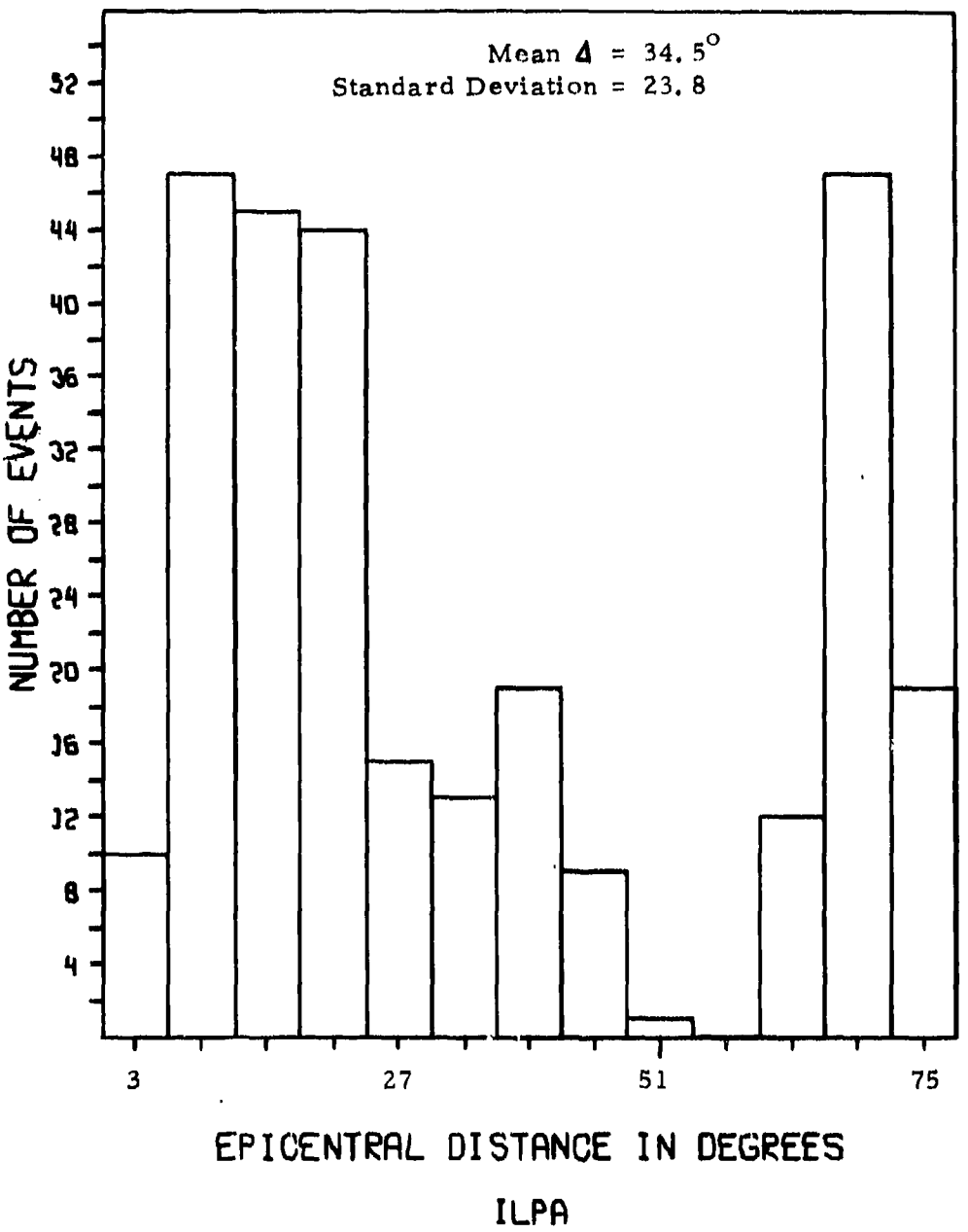

FIGURE III-1

NUMBER OF EVENTS AS A FUNCTION OF EPICENTRAL DISTANCE

The noise data base was formed by searching the NORSAR event lists for time intervals of at least one hour in duration for each day during which no signals would be expected to arrive at ILPA. Segments 4096 seconds in length were processed and visually examined for unreported signals or system malfunctions. If either was observed, a new time interval for that day was selected.

B. METHOD OF DATA PROCESSING AND ANALYSIS

Five basic programs were used to perform the data processing. The first of these carried out a check for incorrect record lengths and a problem we term the "data-shift error," where the data is shifted one byte out of the correct format positions. This gave us an idea of the quality of the data on each tape. With this information we could avoid wasting time trying to process data from unreadable tapes.

The second program was also used to check the data quality. This program checked for parity errors and timing errors, printing out the type of error and the time at which it occurred.

The third program edited the desired time segments from the data tapes, performed quality checks, computed the trace means for the three components of motion of each site, and output these time segments to a permanent hold tape. The quality check part of this program printed out messages indicating the presence of parity errors, timing errors, clipped data, and spiked data. Also printed out is a summary of segment powers, which can be used to find bad sites. (Bad sites are those sites which are dead, contain uncorrectable spikes, or display abnormally high power levels.)

This edit program was created by adapting the search and read subroutines of the Alaskan Long Period Array (ALPA) edit program to handle the ILPA satellite tape format. The ALPA array parameters in the program were replaced with those for ILPA. By adapting this program to

handle ILPA data, all succeeding programs of the array processing package could be applied to the ILPA data edits without modification. The modified edit program was checked by manually decoding hexadecimal dumps of portions of an ILPA tape and comparing the results with the output of the edit program.

The fourth program performed trace mean removal, rotation of the three components of motion from their recorded vertical, north, east (V, N, E) configuration to a vertical, transverse, radial (V, T, R) configuration, and beamforming of the data. By rotating the data, we separate the surface waves recorded on the horizontal components, resulting in two components of Rayleigh motion (V and R) and one component of Love motion (T). Noise samples retained their V, N, E configuration.

The beamforming process performed by this program increases the signal-to-noise ratio by suppressing random noise by a factor approximately equal to the square root of the number of sites used. Three components of motion from a reference site (normally, site 1) and the three beams are output to a permanent hold tape with appropriate annotation. This program was checked by manually decoding a hexadecimal dump of a portion of a data tape and hand-computing the beam output. This was then compared to the output of the beamforming program.

The fifth program bandpass filtered the reference site and beam traces and output plots suitable for analysis.

The data processing method is illustrated in Figure III-2.

Once the data were plotted, signal analysis consisted of determining whether the event was detected on the single-site and beam traces and measuring amplitude and period information on detected events for surface-wave magnitude computations. Signal-to-noise ratios for both single-site and beam data were measured on the bandpass-filtered traces to allow estimation of beamforming gains. All plots were visually checked for malfunctions and mixed signals.

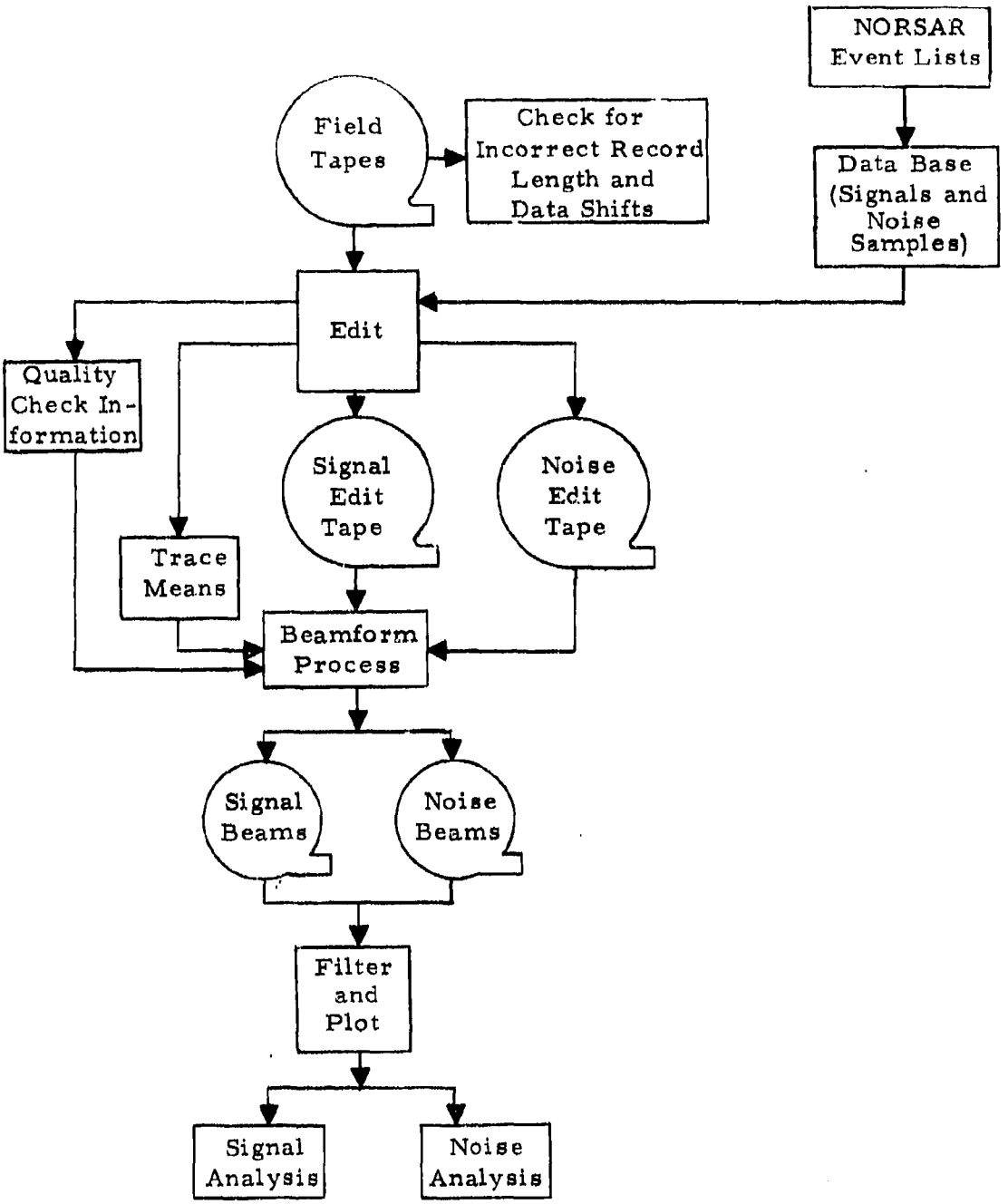

FIGURE III-2

DATA PROCESSING METHOD

SECTION IV
DATA QUALITY

A. DATA TAPE ERRORS

When the ILPA edit program was first created, it was set up to read data in the satellite format exactly as shown in Figure II-2 of Section II. Two problems appeared immediately when the program was tested on ILPA data. First, it was found that each tape has two file marks at the start of the tape which are not mentioned in the format description. Once we were aware of this problem, it was easy to correct by adding a statement in the program to skip over these file marks before beginning to read the data.

The second problem, which we may term the "data-shift" error, is illustrated by Figure IV-1. (In previous discussions of ILPA data, we have referred to this as the "sync error." We here change the name to avoid confusion with a transmission problem at ILPA which is also called the "sync error.") When this data-shift error occurs, we find that all the data has been shifted down one byte in the format. Each data record, according to the satellite data format, is to start with the hexadecimal characters FO and 9A, followed by C9, D3 ('IL') and ending with the characters C8, C8. When the data-shift error occurs, the first hexadecimal characters are C8, FO. The 9A character is in the location reserved for the C9 character (I of 'IL') and so on through the record. This problem occurs frequently. Of the 31 tapes containing May 1976 data, two tapes could not be read and the remaining 29 showed this data-shift error for more than half of the time period recorded. It was found that once this shift occurred, it continued for many hours.

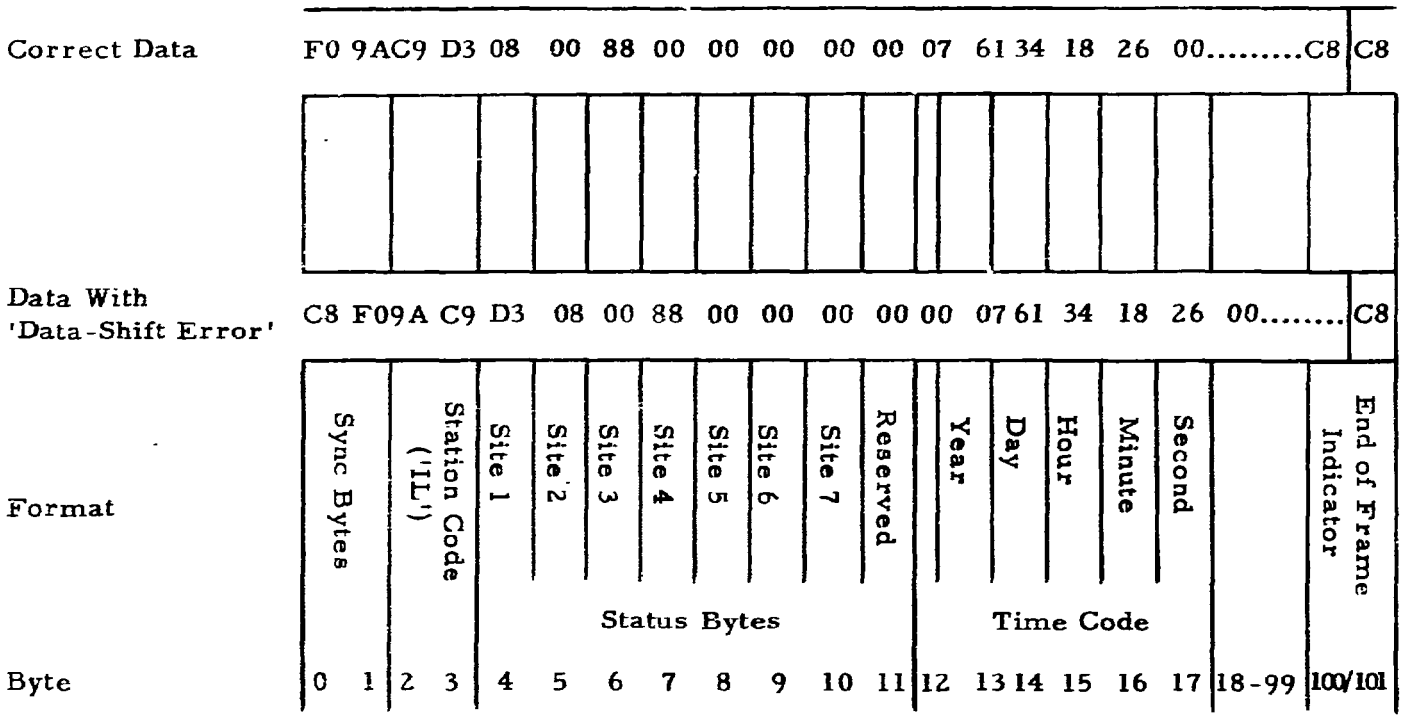

FIGURE IV-1

THE DATA-SHIFT ERROR

The source of this problem is not clear. We sent a copy of one of the ILPA satellite format data tapes to Mr. Wayne Ellis of Texas Instruments Incorporated in Dallas with a list of the times at which we found these data-shift errors. Using hexadecimal dumps of this tape, he was unable to find these errors. Furthermore, during a subsequent trip to ILPA, he was unable to find a cause for these errors. After discussing this problem with an IBM computer engineer in Dallas, he suggested that the source of these errors may lie in the tape transport of the IBM 360/44 located here, causing the computer to misread the inter-record gaps.

Whatever the cause of this problem, we still had to process the data. Therefore, the ILPA edit program was altered so that it first searched for the hexadecimal characters C9,D3 ('IL') and aligned the data relative to their location. Thus, the edit program now sees no difference between correctly formatted data and data containing the data-shift error.

Once we began processing the events of our data base, we began encountering parity errors and timing errors. Using the second data processing program described in Section III, we counted the parity and timing errors on each readable tape. The results are listed in Table IV-1. (Some of the tapes could not be read by this program due to excessive parity or timing errors or missing end-of-tape marks.) Upon encountering a parity error, the edit program prints out an error message indicating the presence and approximate location of the error. It then backspaces the record and attempts to read the data a second time. The data is accepted even if the parity error occurs on the second read. The effect of these parity errors on the data does not appear to be severe. When comparing plots of the data with the parity error listing generated by the edit program, with rare exceptions we do not find that the parity error had any effect on the data. When the parity error occurred in conjunction with a timing error, the plot showed a spike in the data.

TABLE IV-1

SUMMARY OF PARITY AND TIMING ERRORS

Tape	Julian Date	Number of Parity Errors	Number of Timing Errors
1	122-123	10	4
2	122-124	4	4
3	124-125	8	8
4	125-126	27	8
5	126-127	0	11
6	127-128	157	7
8	129-130	1	2
10	131-132	4	7
11	132-133	4	13
12	133-134	0	8
14	135-136	5	2
17	138-139	2	13
18	139-140	0	8
19	140-141	8	10
20	141-142	2	18
21	142-143	4	13
22	143-144	0	8
23	144-145	1	18
24	145-146	2	9
25	146-147	0	5
26	147-148	135	2
27	148-149	0	3
28	149-150	0	5

Upon encountering a timing error (time of sample i + 1 is not equal to time of sample i plus the sample rate), the edit program prints out a message indicating the presence and location of the error, accepts the data associated with the timing error, and continues. As long as there is no timing error at the time the edit is to start, the edit will run, since timing is maintained in the program by a reference timing word. Timing errors for data points following the first point are detected by comparing the time on tape associated with each data point with the reference timing word. We generally see a spike on plots of the data when a timing word error occurs. This implies that the entire data sample is in error and not just the timing word.

B. NUMBER OF GOOD SITES

One indication of the quality of the ILPA data is the number of sites considered to be acceptable for beamforming. A site is rejected from beamforming if any of the following occurs:

- The site is dead.
- One or more components of the site contain uncorrectable spikes or clipped data.
- One or more components contain power surges raising the segment powers more than ten times the power of the preceding and following segments.
- One or more components contain segments with zero power (data drop-outs).
- One or more components contain segment powers consistently much higher than the segment powers at other sites.

The decision to accept or reject a site is made using the edit printout, which lists segment powers for each component of each site edited.

Of the 281 events in the data base, unreadable or missing data prevented the processing of 29 events. The number of sites rejected from beamforming each of the remaining 252 events is summarized in Table IV-2. Since site 1 did not become operational until 5 May, there are only 232 events for this site. Site 3 was not operational during May.

We see from this table that site 6 had the highest rejection rate. In almost all cases, data from this site was rejected due to synchronization errors caused by the relaying of data from site 6 through site 5 to the central recording station. The bulk of these synchronization error rejections occurred on the days 20-23 May and 30-31 May. These errors reduced the site 6 data to meaningless numbers which, when edited, caused many illegal gain codes to be noted. When these errors occurred at site 6, the edit printout showed much higher segment powers than the other sites, with some data drop-outs.

Sites 1, 2, and 4 had approximately the same rejection rate. The reasons for rejecting these sites were most commonly uncorrectable spikes and power surges. Sites 5 and 7 had the lowest rejection rates. The reason for rejecting these sites was most commonly that one component contained segment powers consistently much higher than the segment powers at other sites.

C. SUMMARY OF OBSERVATIONS ON DATA QUALITY

The remarks made to this point on the quality of the ILPA data may lead one to believe that the data quality is poor. However, as was mentioned earlier, we have found ways of coping with most of the problems we found. The data-shift error was easily corrected by aligning the data on the 'IL' characters. Except when timing errors occur at the desired edit start time, these errors do not interfere with the running of the edit program. When timing errors do occur at the edit start time, we change the edit start time to a time a few minutes later. Since we always edit a noise gate before the desired signal, this change in the edit start time does not affect the signal.

TABLE IV-2

SUMMARY OF SITE REJECTION STATISTICS

Site *	Number Of Times Rejected	Total Number of Times Site Was Available	Percent Rejected
1	19	232	8.2
2	20	252	8.0
4	21	252	8.3
5	8	252	3.2
6	37	252	14.7
7	6	252	2.3

*Site 3 was not operational during May 1976.

The synchronization errors affecting site 6 are handled by rejecting this site when beamforming. The only effect this has is to decrease the signal-to-noise ratio gain which the beamforming provides.

Overall, we judge the ILPA data quality to be fairly good. Of the 281 events of our data base, 84.0 percent were successfully processed, 1.8 percent were lost due to no data being recorded, 5.3 percent were lost to uncorrectable malfunctions, and 8.9 percent were lost to unreadable data. The uncorrectable malfunctions were predominantly data spikes caused by bad data associated with timing errors.

SECTION V
SIGNAL ANALYSIS

A. SIGNAL-TO-NOISE RATIO GAINS DUE TO BEAMFORMING

When the data recorded at the individual sites of an array are formed into beams, the signal-to-noise ratio of each component is increased due to suppression of noise. In the ideal case, the noise is purely random and is suppressed by a factor approximately equal to the square root of the number of sites used in the beamforming process. In practice, the noise is composed of a random component and a propagating non-random component. This propagating component is suppressed to a lesser degree than the random component, the amount of suppression depending on how far off the beamforming azimuth its azimuth lies. Also, the beamforming process suppresses the signal to some extent. This is dependent on how accurate the computed time delays used to time-align the individual traces are. In particular, at some point close to the array, the plane-wave assumption used to compute these time delays must break down.

To obtain a first estimate of the signal-to-noise ratio gains we may expect from the beamforming process, we selected a small suite of events which were detected on both the reference site and beam traces and contained only noise in the time gate immediately preceding the signal arrival time. The signal-to-noise ratio for each component of the reference site and beam traces were then computed using the equation:

$$S/N\ (dB) = 20. * LOG_{10} \frac{\text{zero-peak amplitude}}{\text{RMS noise}}$$

where "zero-to-peak amplitude" is the amplitude of the largest peak of the signal waveform and "RMS noise" is measured in the time gate immediately preceding the signal arrival. The gain due to beamforming is then simply the difference between the beam signal-to-noise ratio and the reference site signal-to-noise ratio.

The results in Table V-1 are grouped on the basis of epicentral distance. The values in the column headed "optimum gain" were computed from the following equation:

$$\text{Optimum Gain (dB)} = 20. * \text{LOG}_{10} \sqrt{\text{number of sites}}$$

where "number of sites" is the average number of sites used in beamforming. We see in this table that beamforming gains for the vertical and radial components of events with epicentral distances less than ten degrees are very low. This indicates that the plane-wave assumption used in beamforming to compute time delays fails for events with epicenters less than ten degrees from the array. The high gain value for the corresponding transverse component is not yet understood.

The mean gains for the other ranges of epicentral distances remain fairly constant. This implies that the plane-wave assumption holds for events with epicentral distances greater than ten degrees.

Comparing the mean gains in Table V-1 with the corresponding optimum gains, we see that in general the mean gains are lower than the optimum gains. This implies that some of the noise is propagating, since, as was described earlier, propagating noise is suppressed by beamforming to a lesser degree than is random noise.

An interesting feature of the data in Table V-1 is that the radial component gains are lower than the vertical component gains. In Table

TABLE V-1

SIGNAL-TO-NOISE RATIO GAINS DUE TO BEAMFORMING

Δ Range	Number of Samples	Average Number Of Sites	dB Gains			Optimum Gain
			V	T	R	
0°-10°	4	4.50	-0.29	6.05	-2.93	6.53
10°-20°	13	5.69	7.67	4.50	3.85	7.55
20°-40°	10	5.30	6.40	2.93	1.50	7.24
$>40^{\circ}$	12	5.42	4.33	2.76	3.95	7.34
10°-80°	35	5.49	6.17	3.70	3.46	7.39

V-2 we have separated the signal-to-noise ratio gains into the signal-to-noise gain due to RMS noise suppression and the signal-to-noise ratio loss due to peak signal suppression. From the data in this table we see that the difference in signal-to-noise ratio gain between the vertical and radial components is due to both lower RMS noise suppression and greater signal suppression on the radial component, with the greater signal suppression being the dominant factor. The lower RMS noise suppression on the radial component in conjunction with lower RMS noise suppression on the transverse component relative to the vertical component implies that there is more propagating noise on the horizontal components than on the vertical components. We do not as yet understand the greater peak signal suppression on the radial components.

B. SHORT-PERIOD ILPA DETECTION CAPABILITY

During the current contract period there was no plan to process ILPA short-period data. However, we were able to review develocorder films of ILPA short-period data for the first ten days of May 1976. This period covered events 1 to 45 of our data base. The detection results presented here are based on the short-period vertical component of site 7. (This is the short-period component which is recorded on the ILPA satellite format tapes. Thus, our results are indicative of the detection capability of the unfiltered data available to us on these tapes.) The detection criteria for these data are:

- Presence of an impulsive waveform occurring within $\pm$ 20 seconds of the predicted P-wave arrival time.
- Waveform under consideration is at least 12 dB above the preceding noise.

The results of this very brief analysis are presented in Figure V-1. The upper portion of this figure shows the distribution of detected and

TABLE V-2

RMS NOISE SUPPRESSION AND PEAK SIGNAL SUPPRESSION
DUE TO BEAMFORMING

	Δ Range	V	T	R
RMS Noise Suppression	0°-10°	5.56	7.32	4.26
Due To Beamforming (dB)	10°-80°	6.79	4.74	6.07
Peak Signal Suppression	0°-10°	5.85	1.27	7.19
Due To Beamforming (dB)	10°-80°	0.62	1.04	2.61
Resultant Change In	0°-10°	-0.29	6.05	-2.93
Signal-To-Noise Ratio (dB)	10°-80°	6.17	3.70	3.46

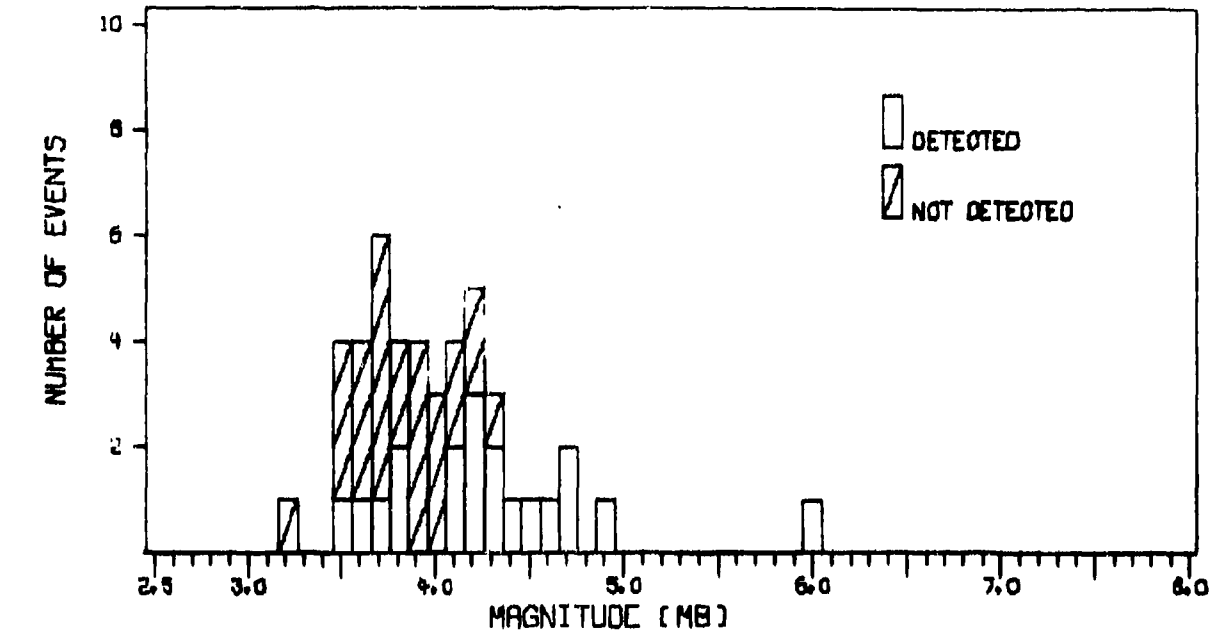

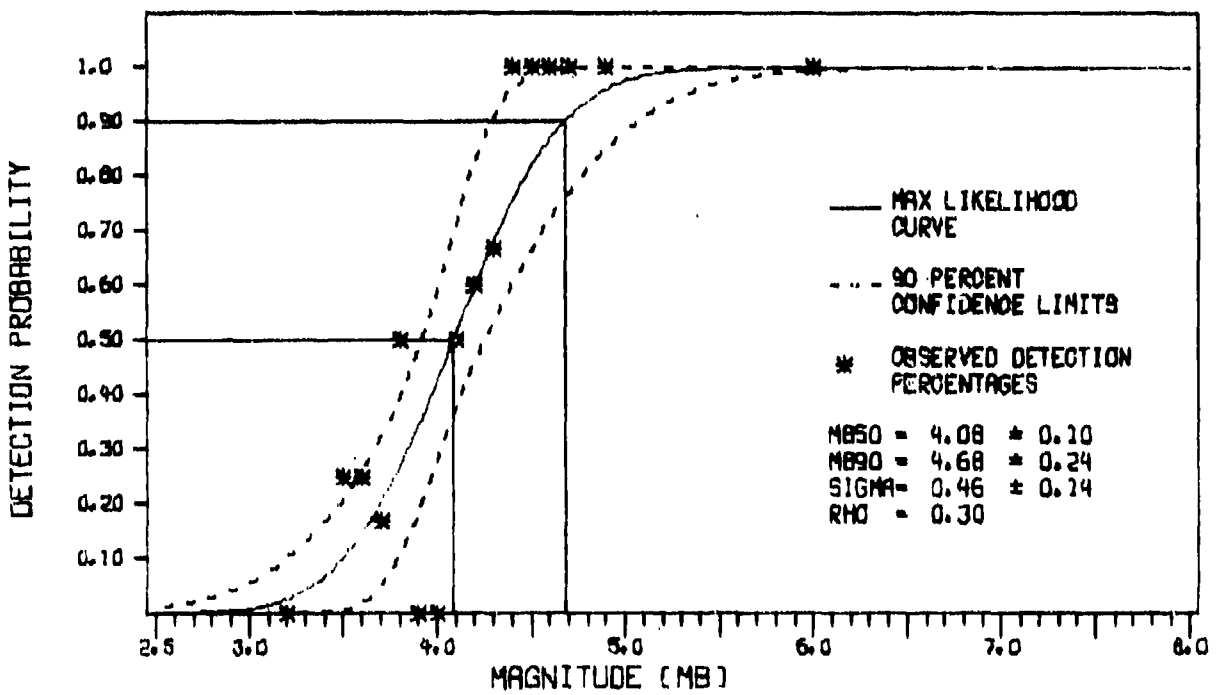

FIGURE V-1

ILPA SHORT-PERIOD DETECTION STATISTICS

non-detected events as a function of bodywave magnitude (m_b). The lower portion of this figure shows the maximum likelihood curve fitted to these detection statistics (Ringdal, 1974).

The subset of events used in this computation of detection capability has a mean epicentral distance of 37.1 degrees with a standard deviation of 23.8 degrees. These values are essentially the same as those for entire data base. From Figure V-1, we see that these events give us an ILPA short-period 50 percent detection threshold estimate of 4.08 m_b units.

C. INDIRECT ESTIMATES OF LONG-PERIOD DETECTION CAPABILITY

It is possible to derive detection threshold magnitudes from ambient noise levels, since detection of a seismic event depends on the signal-to-noise ratio at the recording station. Unger (Unger, 1974) developed the theoretical background for this method and tested it on Very Long Period Experiment data. In this method, it is assumed that an event can be detected when its maximum amplitude exceeds that of the surrounding noise by a certain margin. The detection capability estimation algorithm which Unger develops is:

$$M_{s\,50} = \text{MEAN LOG AMP} - \log_{10} T_o * G(T_o) + \log_{10} \Delta_o + d(T_o) - \overline{b} + C$$

where

$M_{s\,50}$ = the 50 percent surface wave detection threshold,

MEAN LOG AMP = the mean of the logarithms of the maximum peak-to-peak seismometer output noise amplitudes,

T_o = the geometric mean of the period of the maximum signal amplitude,

$G(T_o)$ = the instrument response correction for period T_o, taken from instrument response curves supplied to us by Wayne Ellis of Texas Instruments Incorporated in Dallas, Texas,

Δ_o = the geometric mean of the signal epicentral distances,

$d(T_o)$ = the station magnitude difference due to period T_o,

$\bar{b}$ = the mean station bias,

C = 1.12 + the detection criterion margin.

We used 17 noise samples from May to compute MEAN LOG AMP. The parameter T_o was selected to be 20 seconds, since this period was more often observed in detected signals than either 30 seconds or 40 seconds. $G(T_o)$ was then the instrument response correction at 20 seconds picked from the long-period instrument response curve. The parameter Δ_o was varied from 10^o to 100^o in 10^o increments to give us a table of $M_{s\ 50}$ versus epicentral distance. The parameter $d(T_o)$ was picked from the plot of magnitude difference versus period found in Unger's report (Unger, 1974). For a period of 20 seconds and a continental path, this parameter has the value of -0.01. Since we had no previous knowledge of the mean station bias, $\bar{b}$ was assumed to be zero. The detection criterion was set at a factor of two, i.e., the maximum signal amplitudes must be twice the maximum noise amplitudes, giving us $C = 1.12 + 0.301 = 1.421$. The results of these computations are given in Table V-3.

D. DIRECT ESTIMATES OF LONG-PERIOD DETECTION CAPABILITY

In this subsection, we shall examine the direct estimates of detection capability of the reference site and beam data. The criteria which determine whether an event was detected are:

- The presence of signal dispersion in the signal gate,
- A peak in the dispersed wavetrain 3 dB or more above any peak outside the dispersed wavetrain and inside a 20-minute time gate centered at the expected peak occurrence time,

TABLE V-3

INDIRECT ESTIMATES OF LONG-PERIOD DETECTION CAPABILITY
VERTICAL COMPONENT

Δ°	Reference Site		Beam	
	M_s50	m_b50	M_s50	m_b50
10°	2.78	3.91	2.50	3.74
20°	3.08	4.08	2.80	3.92
30°	3.26	4.19	2.98	4.02
40°	3.38	4.26	3.10	4.09
50°	3.48	4.31	3.20	4.15
60°	3.56	4.36	3.28	4.20
70°	3.63	4.40	3.35	4.24
80°	3.68	4.43	3.40	4.27
90°	3.74	4.47	3.46	4.30
100°	3.78	4.49	3.50	4.33

m_b50 is calculated from $M_s = 1.72\ m_b - 3.94$
(Table V-5 vertical component 20-second period)

- The onset of the signal occurs within $\pm$ 180 seconds of the expected signal onset time.

Of the 252 events which were successfully processed, we found no events which we designated as detected which did not fulfill the first two criteria. Occasionally, the third criterion was not fulfilled, the observed waveform arriving later than expected. In such cases, the event lists were checked to ensure that the detected waveform was not due to some other event. If no other event could be found whose surface waves would arrive at that time, the event under consideration was called a detection.

We first calculated the detection capability of the array using all events of the data base. In this case, mixed events, events containing malfunctions, events for which no data was recorded, and events for which the data was unreadable were all counted as non-detections. The results for this case are shown in Figures V-2 to V-4. The upper portion of each figure shows the distribution of detected and non-detected events as a function of bodywave magnitude (m_b). The lower portion of each figure shows the maximum likelihood curve fitted to these detection statistics. In the figure, "MB50" denotes the 50 percent detection threshold, "MB90" denotes the 90 percent detection threshold, "SIGMA" is related to the slope of the maximum likelihood curve, and "RHO" denotes the quality of the results (Ringdal, 1974).

These figures tell us the absolute probability of detecting an event with given m_b from Eurasia. For example, the 50 percent detection probability is at m_b equal to 4.55 for Rayleigh waves and 4.48 for Love waves.

We next consider the case where only events for which a detection/non-detection decision could be made were included in the detection statistics. This gives us the conditional detection probability curves shown in Figure V-5 for reference site data and in Figure V-6 for beam data. (The term 'conditional' means that the probability curves are computed under the condition that a clear detection/non-detection decision be possible for each event considered.) We do not show the corresponding plots for the transverse

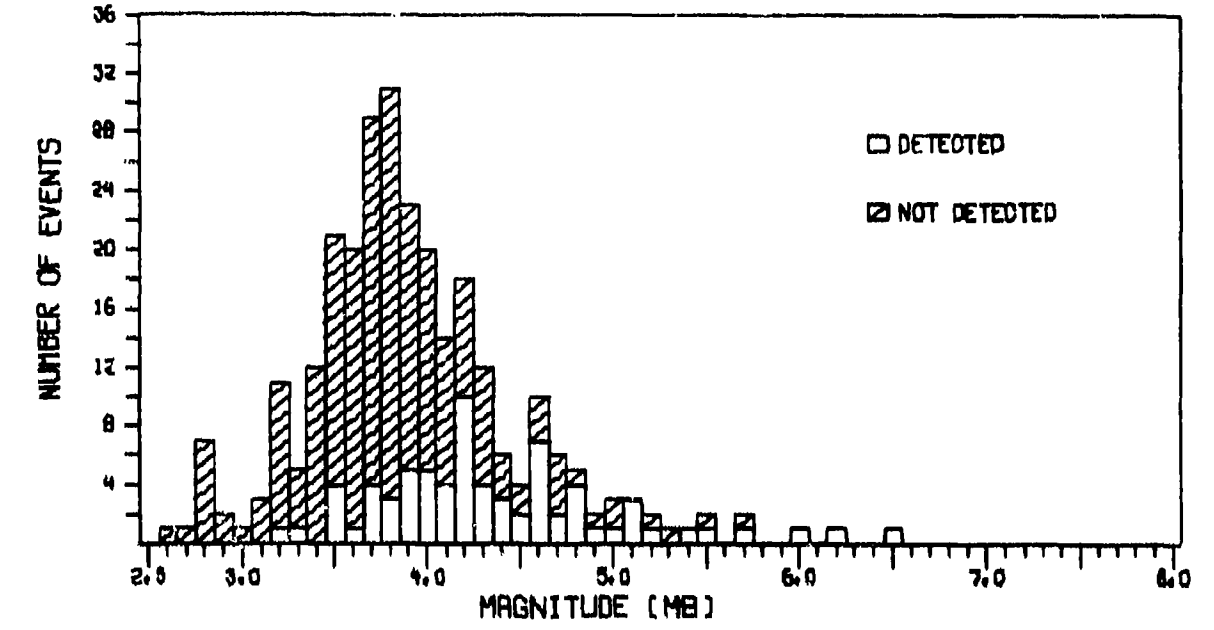

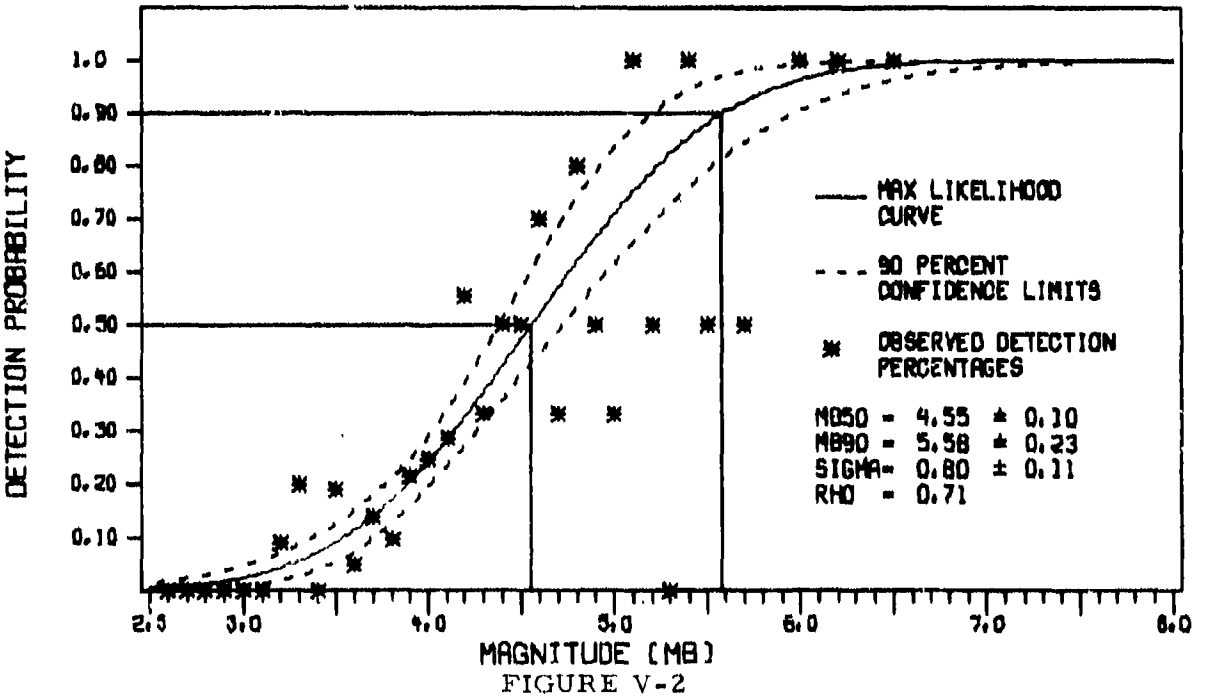

FIGURE V-2

ILPA LONG-PERIOD VERTICAL COMPONENT DETECTION STATISTICS:
MIXED EVENTS, EVENTS CONTAINING MALFUNCTIONS, AND
EVENTS FOR WHICH NO DATA WAS RECORDED
TREATED AS NON-DETECTIONS

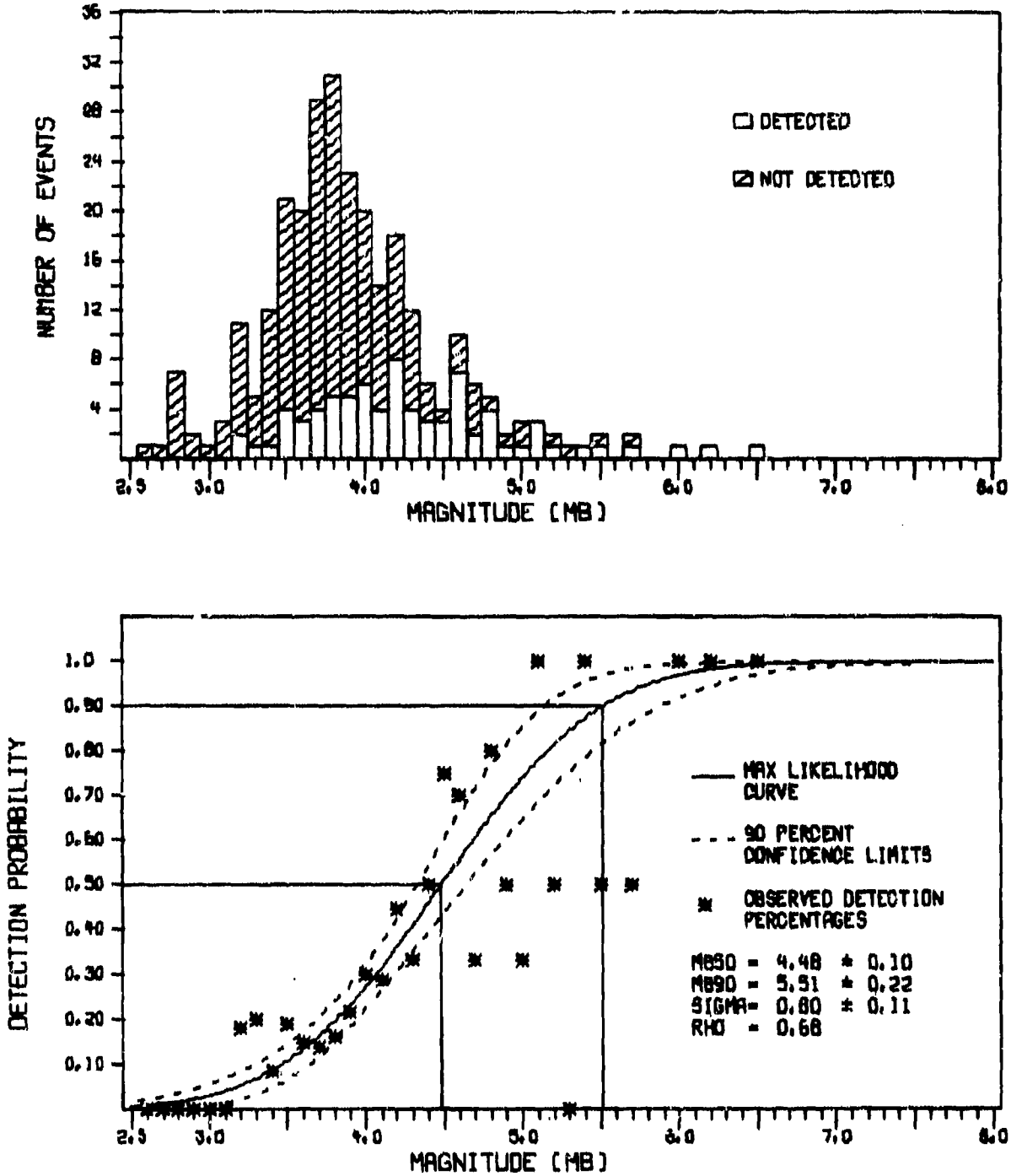

FIGURE V-3

ILPA LONG PERIOD TRANSVERSE COMPONENT DETECTION STATISTICS: MIXED EVENTS, EVENTS CONTAINING MALFUNCTIONS, AND EVENTS FOR WHICH NO DATA WAS RECORDED TREATED AS NON-DETECTIONS

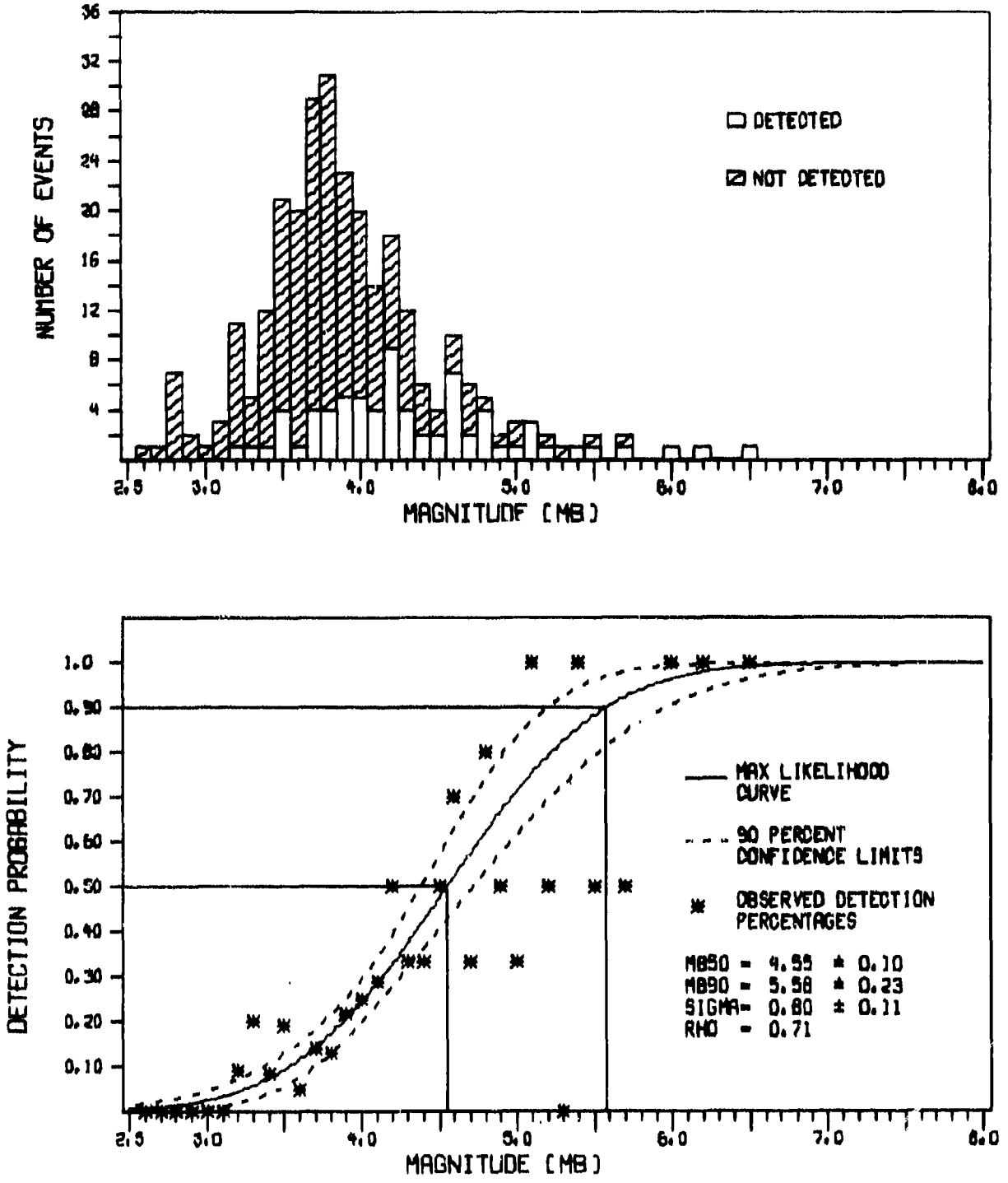

FIGURE V-4

ILPA LONG PERIOD RADIAL COMPONENT DETECTION STATISTICS: MIXED EVENTS, EVENTS CONTAINING MALFUNCTIONS, AND EVENTS FOR WHICH NO DATA WAS RECORDED TREATED AS NON-DETECTIONS

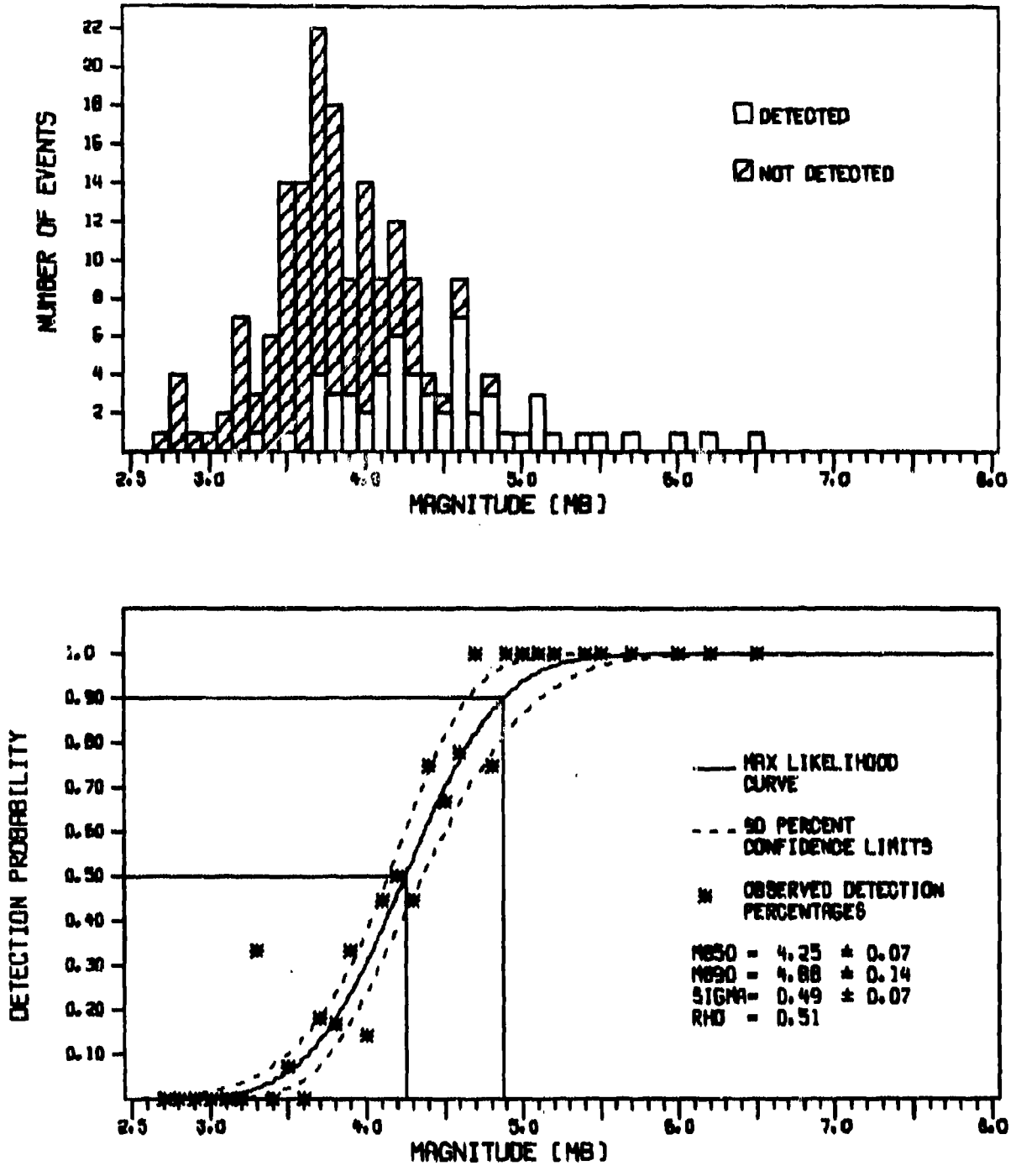

FIGURE V-5

ILPA REFERENCE SITE VERTICAL COMPONENT DETECTION STATISTICS

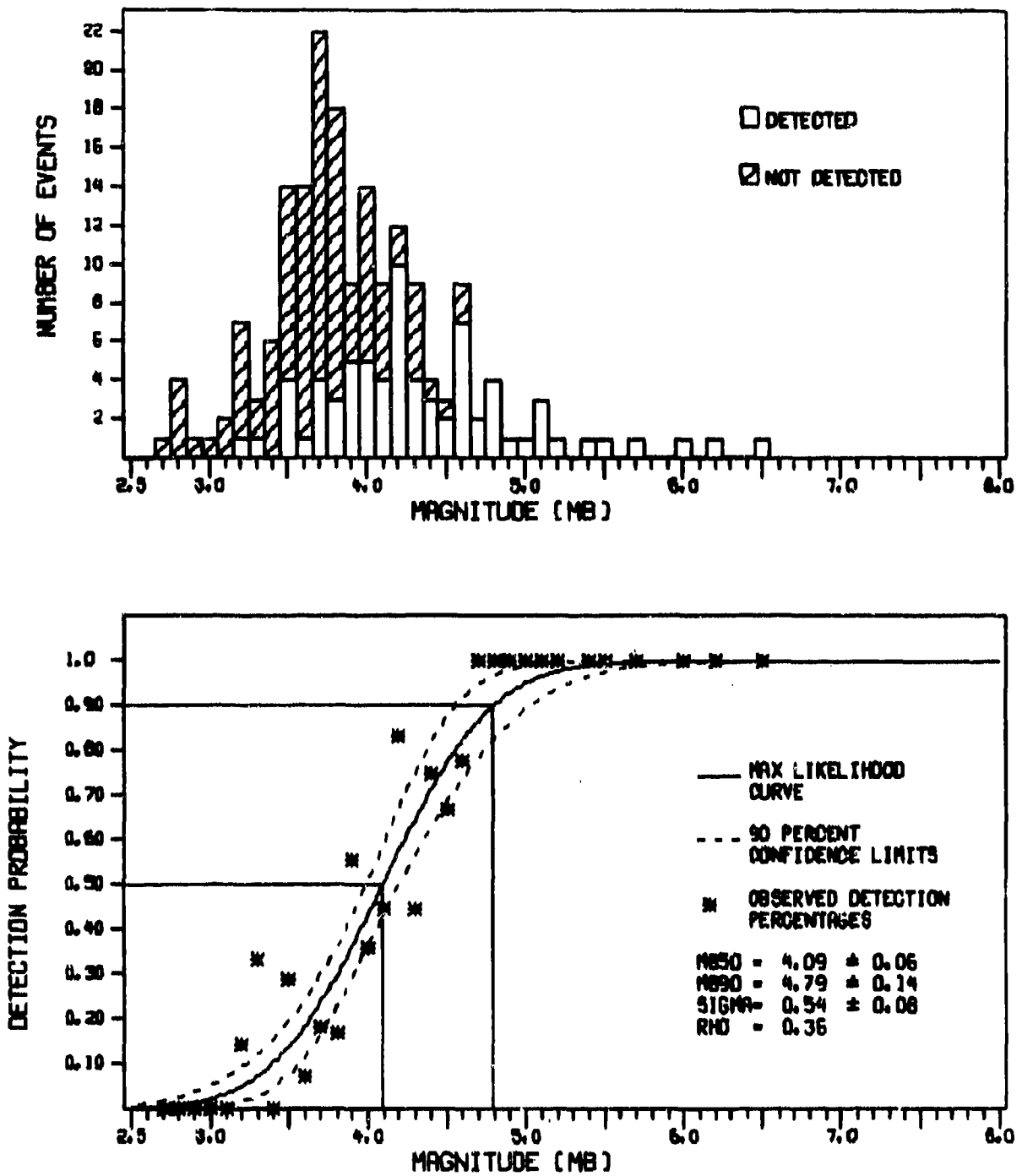

FIGURE V-6

ILPA BEAM VERTICAL COMPONENT DETECTION STATISTICS

and radial components because the results are essentially the same. The detection capability is summarized in Table V-4. We note that the indirect estimates were taken from Table V-3 using the mean epicentral distance for the data base (34.5°). These indirect estimates are conditional detection capability estimates since the assumption that there are no malfunctions, mixed signals, missing data, or unreadable data is implicit in their computation.

The following points concerning the data in Table V-4 can be made:

- Malfunctions, mixed signals, missing data, and unreadable data cost us 0.45 m_b units in detection capability.
- The indirect detection estimates are in close agreement with the direct estimates.
- Beamforming lowers the 50 percent detection threshold by approximately 0.15 m_b units on all components.

Although the data base was too small to regionalize the detection capability, it was possible to approximate this by separating the events into three groups based on epicentral distance. These groups are near field ($0° \leq \Delta < 20°$), near teleseismic ($20° \leq \Delta < 50°$), and far teleseismic ($50° \leq \Delta < 80°$). The maximum likelihood detection curves for these three cases are shown in Figures V-7 to V-9. Again, these curves give conditional detection probabilities, since all mixed events, events with malfunctions, events with missing data, and events with unreadable data have been removed from the detection statistics. As before, we show only the vertical component results, since the results for the horizontal components were essentially the same.

Up to this point we have discussed detection capability in terms of individual components. We will now look at the combined detection capability of the components. (Again, we will use conditional detection probabilities, i.e., all mixed events, events for which no data was recorded, events which contained malfunctions, and events for which the data was unreadable have been removed from the detection statistics.) In Figure V-10 we show the

TABLE V-4

SUMMARY OF DETECTION CAPABILITY INFORMATION
50 PERCENT BODYWAVE MAGNITUDE (m_b) DETECTION CAPABILITY

Component	Absolute Detection Capability	Conditional Detection Capability			
		Indirect Estimates		Direct Estimates	
	Beam	Reference Site	Beam	Reference Site	Beam
Vertical	4.55	4.22	4.05	4.25	4.09
Transverse	4.48	*	*	4.16	4.04
Radial	4.55	*	*	4.24	4.09

*Not Measured

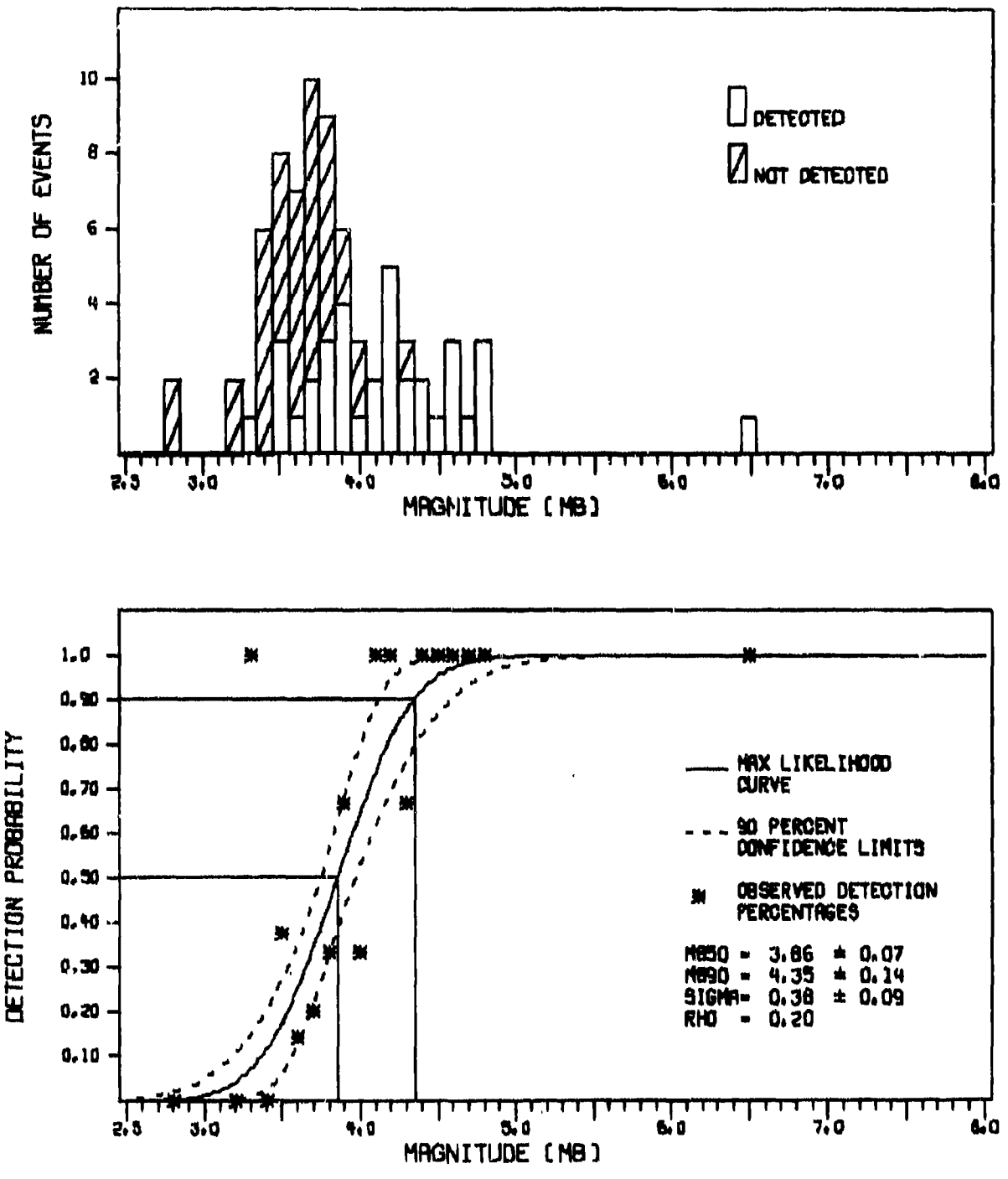

FIGURE V-7

ILPA BEAM VERTICAL COMPONENT DETECTION STATISTICS
$0^{\circ} \leq \Delta < 20^{\circ}$

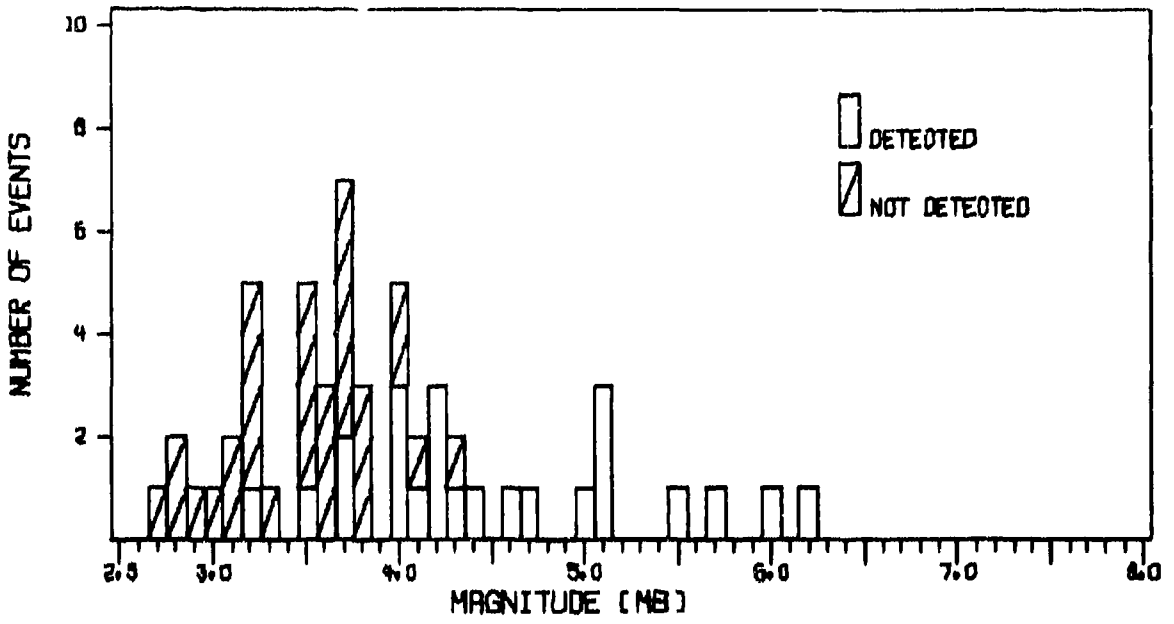

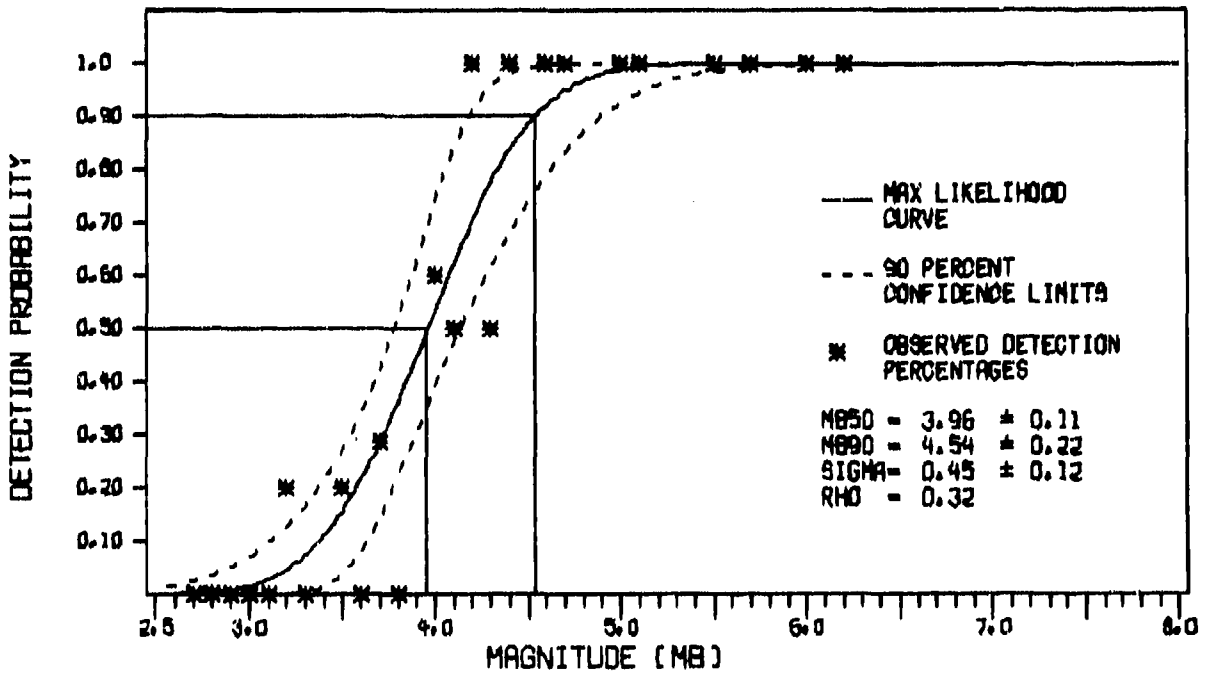

FIGURE V-8

ILPA BEAM VERTICAL COMPONENT DETECTION STATITICS
$20^{o} \leq \Delta < 50^{o}$

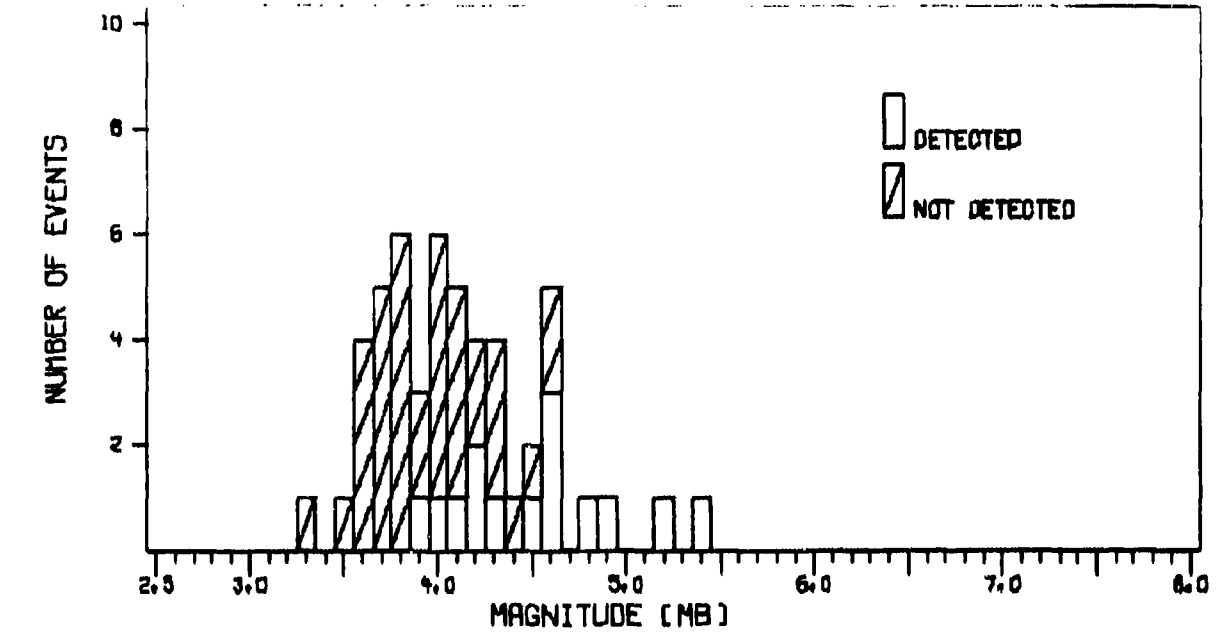

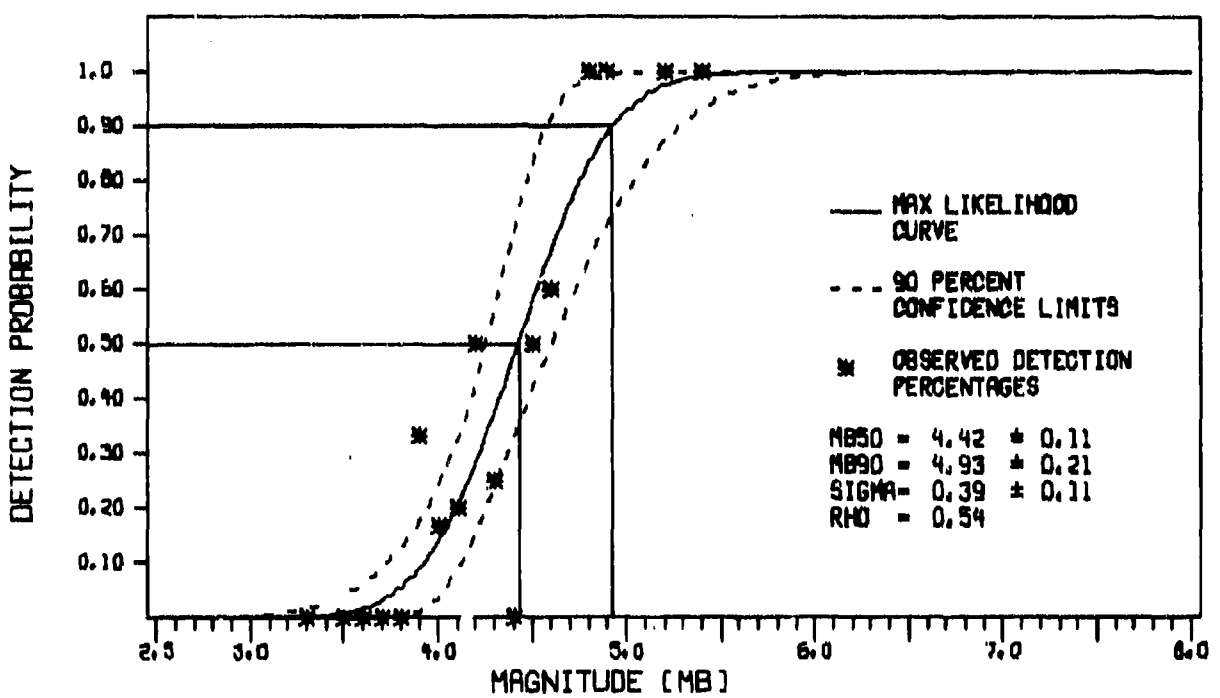

FIGURE V-9

ILPA BEAM VERTICAL COMPONENT DETECTION STATISTICS
$50^{\circ} \leq \Delta < 80^{\circ}$

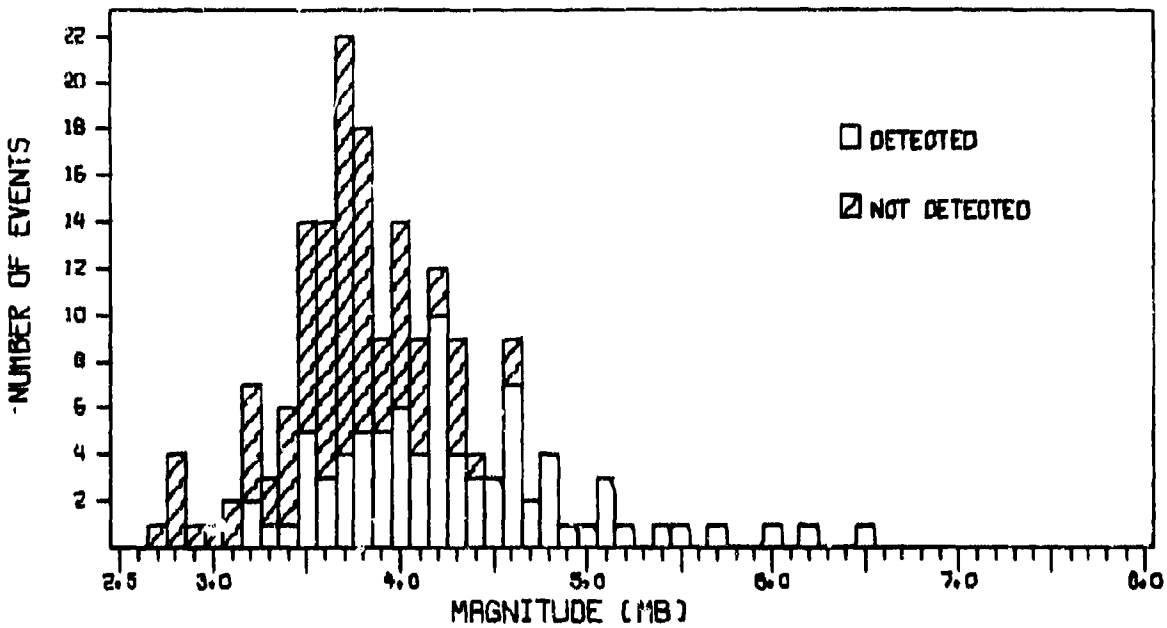

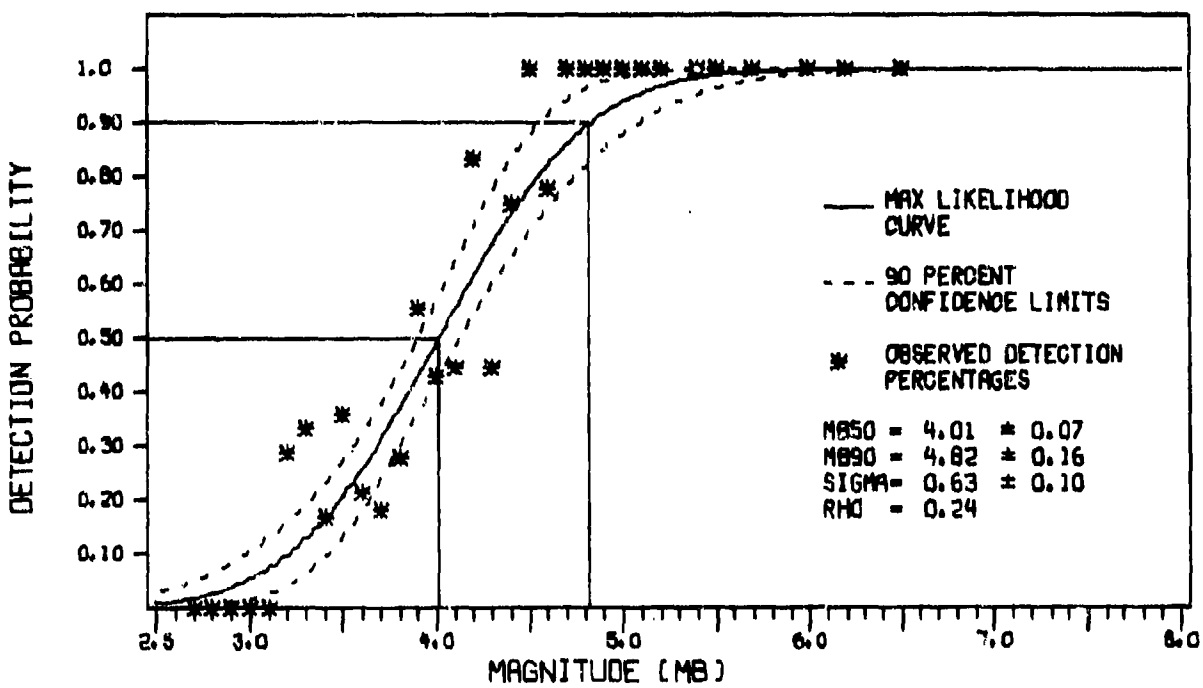

FIGURE V-10

ILPA BEAM DETECTION STATISTICS: DETECTION ON ONE COMPONENT REQUIRED TO DECLARE AN EVENT DETECTION

beam detection statistics for the case where an event is declared to be detected if it is detected on one or more component. The 50 percent detection threshold for this case is at $m_b = 4.01$. We might call this case our optimistic detection capability estimate.

In Figure V-11 we show the beam detection statistics for the case where an event is declared to be detected only if it is detected on all three components. The 50 percent detection threshold for this case is at $m_b = 4.13$. We might call this case our conservative detection capability estimate.

E. $M_s - m_b$ RELATIONSHIP AT ILPA

We cannot estimate the discrimination capability of ILPA since our data base does not contain any presumed explosions. We can, however, make a start on this portion of the ILPA evaluation by describing the earthquake $M_s - m_b$ relationships at this array.

Surface wave magnitudes (M_s) were computed using the equation:

$$M_s = \text{Log}_{10}\left[\frac{A}{\text{S. F.} * G * Q * T}\right] + \text{Log}_{10}\Delta + 1.12$$

where

A = Peak-to-peak amplitude measured in inches on the plot of the event,

S. F. = The plot scale factor in inches per computer count,

G = The instrument response correction factor,

Q = The quantization rate (20.951 cc/mμ),

T = The period at which the amplitude A was measured,

Δ = The epicentral distance of the event.

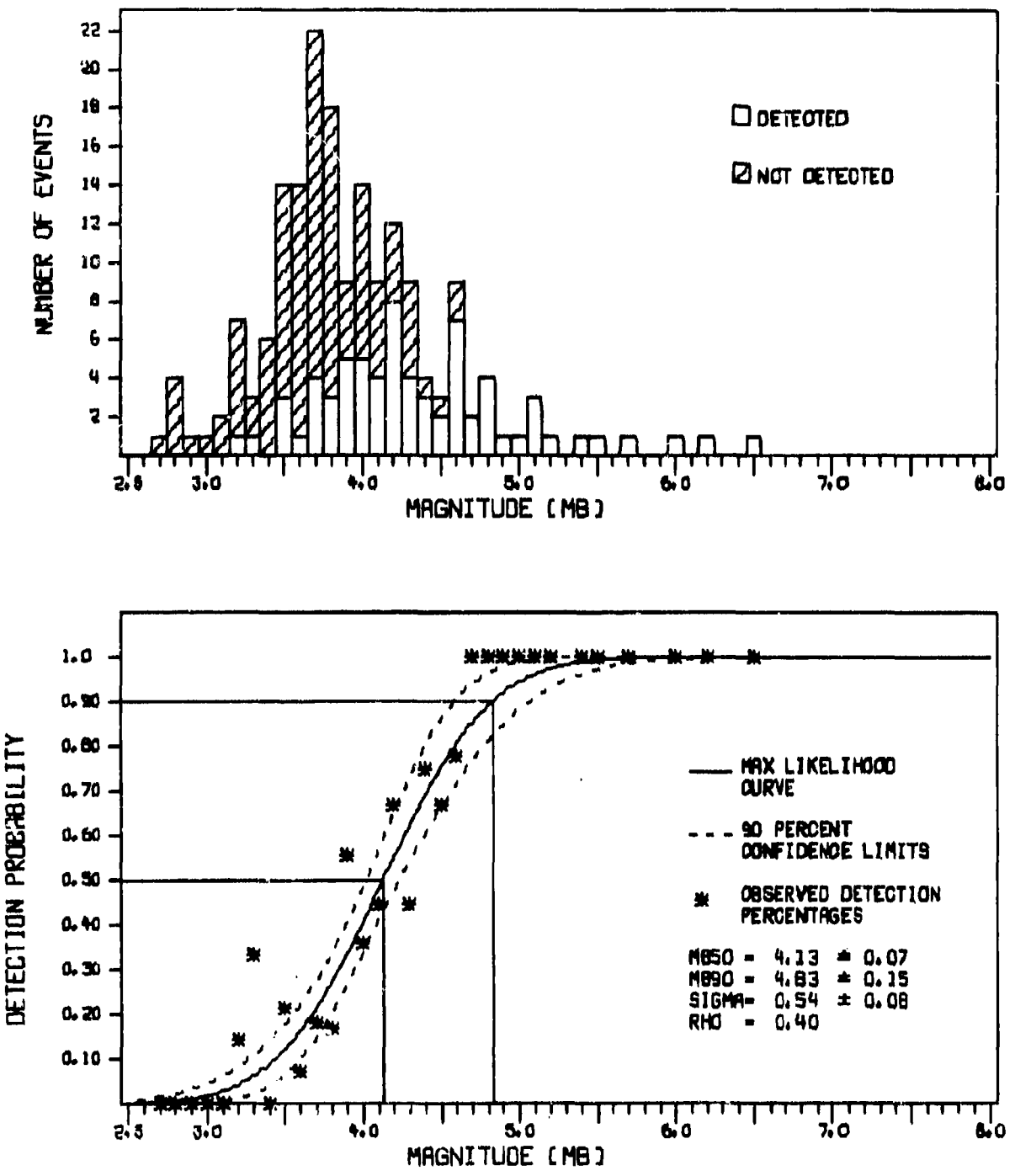

FIGURE V-11

ILPA BEAM DETECTION STATISTICS: DETECTION ON ALL COMPONENTS REQUIRED TO DECLARE AN EVENT DETECTION

The normalized instrument response curve from which G was taken is shown in Figure V-12. This curve was created by averaging the individual site instrument response curves supplied by Wayne Ellis of Texas Instruments Incorporated in Dallas. (One normalized instrument response curve for each site was supplied. Since this was the only information we had, we used this curve for all three components.) The vertical bars on the curve show plus or minus one standard deviation at each of the measurement points.

Wherever possible, M_s was measured at periods of 20, 30, and 40 seconds. Figures V-13 to V-15 show the M_s-m_b data with M_s measured at 20 seconds on the vertical, transverse, and radial beams, respectively. The fit to the data points shown in each figure treats neither variable as dependent, minimizing the perpendicular distance from the line to the data points.

In Table V-5 we list the slope and intercept of these M_s-m_b fits, where a and b are the coefficients in the equation:

$$M_s = a\, m_b + b.$$

We used this information to construct Figure V-16, showing the M_s-m_b fits at 20, 30, and 40 seconds for each component of motion. These plots show that, on the average, the 30 second M_s is lower than the 20 second M_s and the 40 second M_s is lower than both the 20 second and 30 second M_s.

At this point we are in need for depth information for the earthquakes and a suite of presumed explosions to carry out the evaluation of the ILPA discrimination capability. The depth information will be used to eliminate deep events from the data base. These events should be removed, since they tend to generate lower surface waves than do the shallow events. Thus, their removal will lower the variance of the earthquake population about the M_s-m_b earthquake fit. The presumed explosion M_s-m_b data would then be plotted, and we could finally determine the quality of this discriminant.

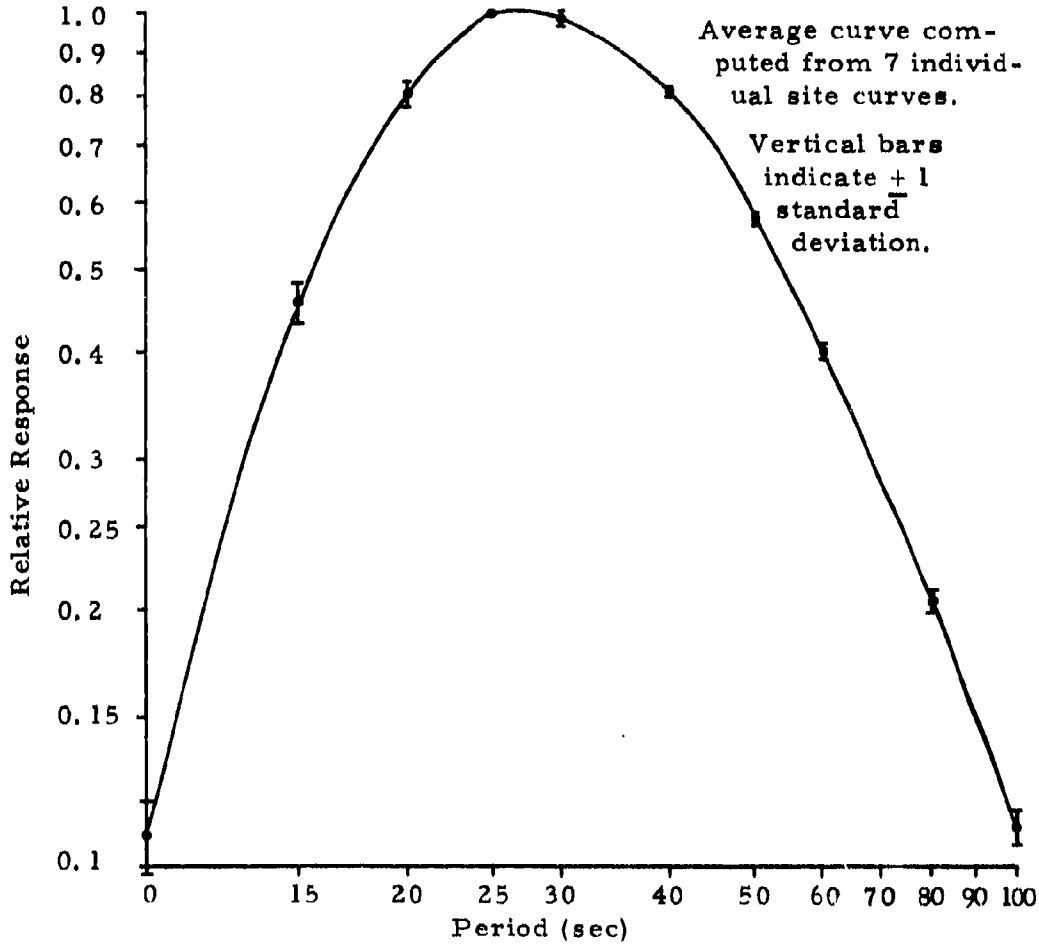

FIGURE V-12

ILPA INSTRUMENT RESPONSE
NORMALIZED AT 25 SECONDS

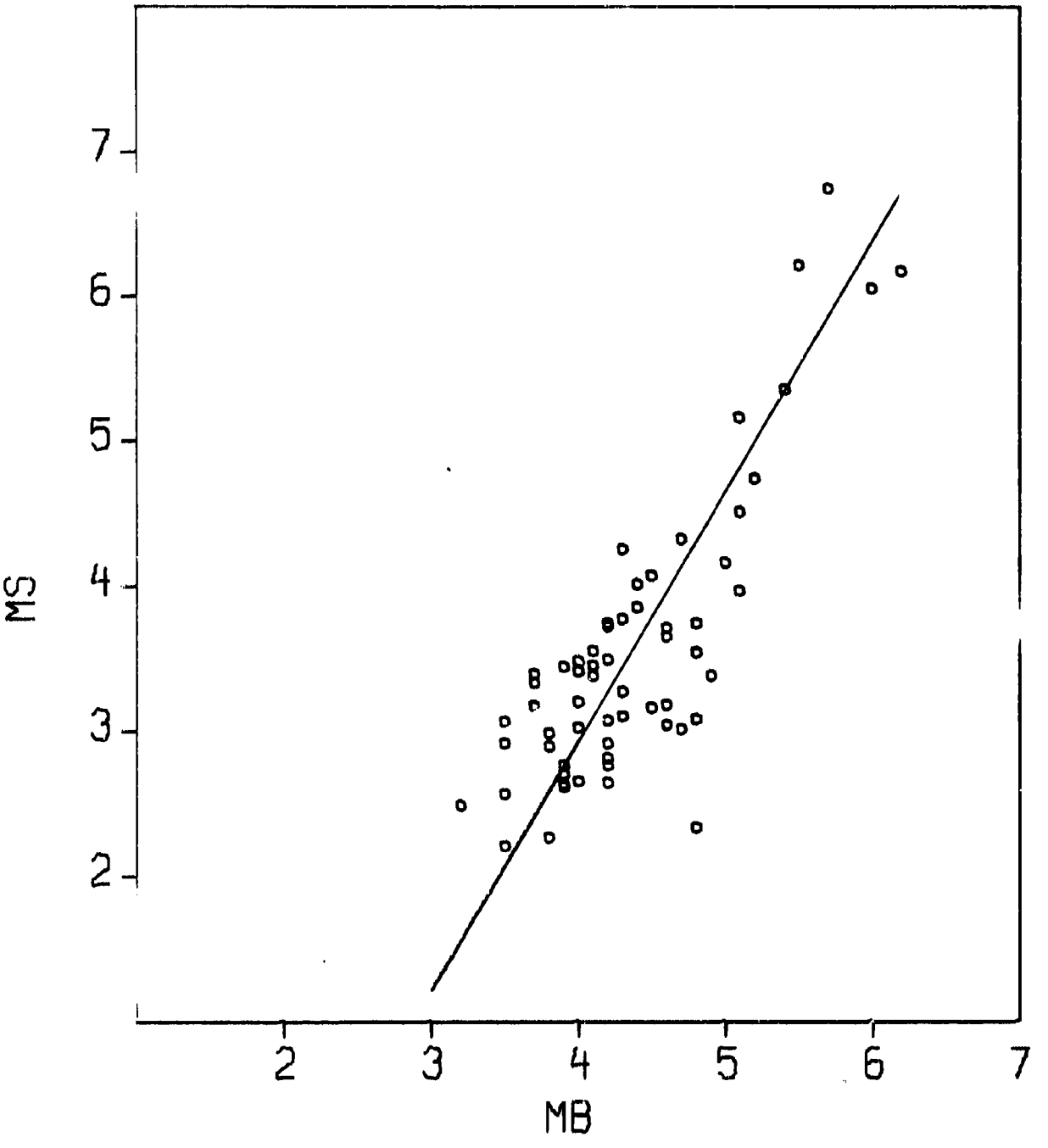

FIGURE V-13

ILPA VERTICAL COMPONENT M_s-m_b RELATIONSHIP
FOR 20 SECOND M_s

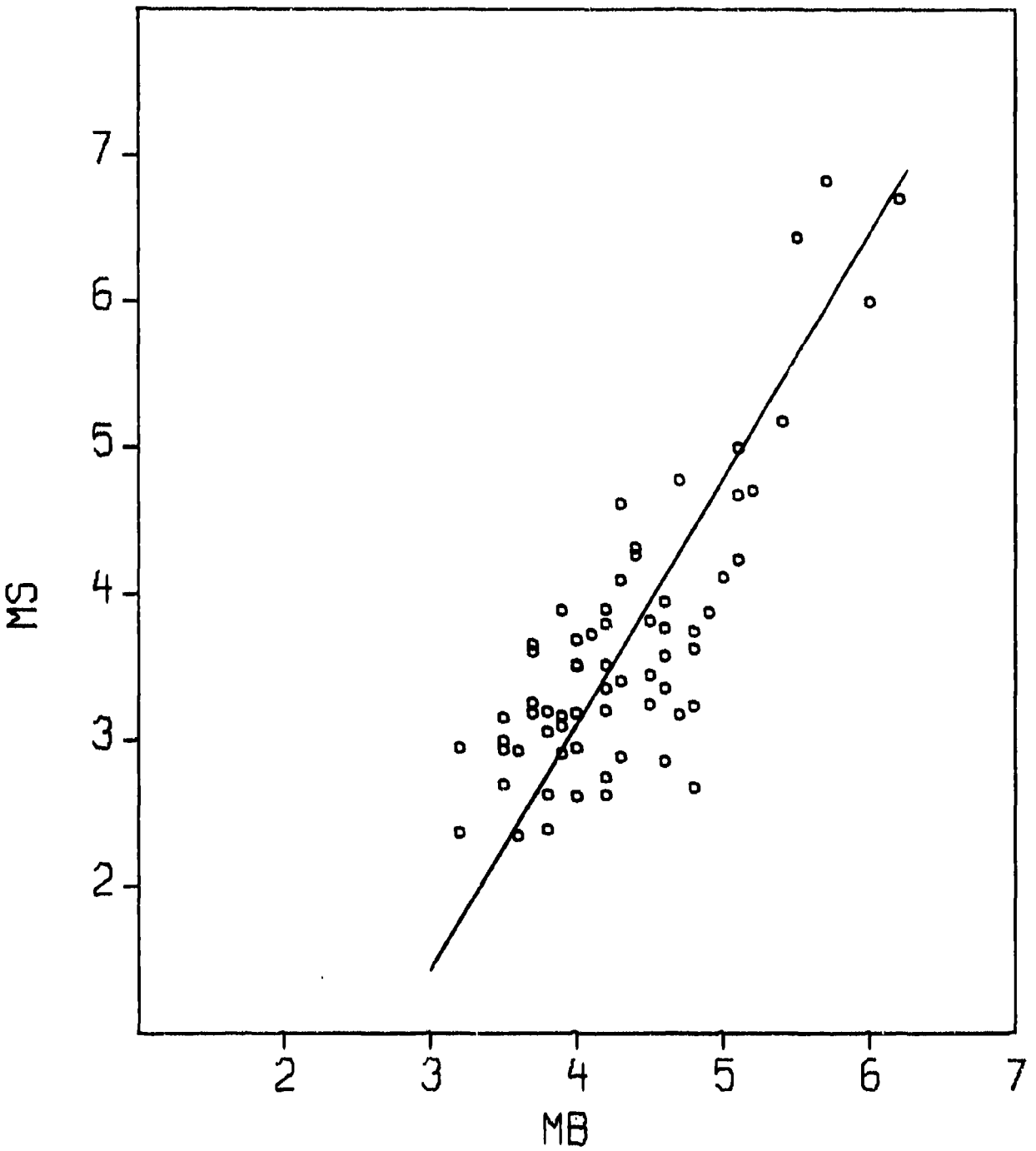

FIGURE V-14

ILPA TRANSVERSE COMPONENT M_s-m_b RELATIONSHIP
FOR 20 SECOND M_s

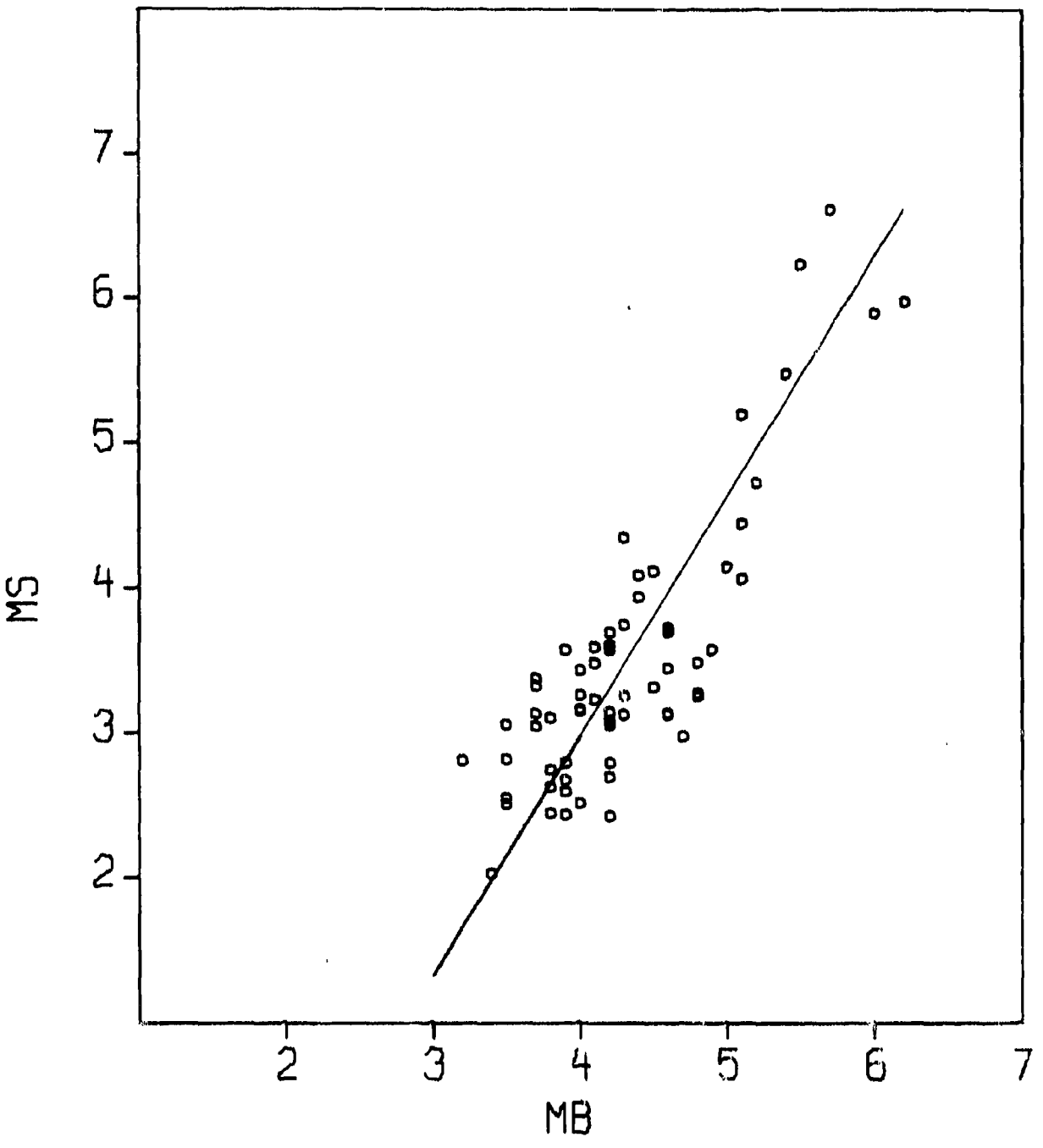

FIGURE V-15

ILPA RADIAL COMPONENT M_s-m_b RELATIONSHIP
FOR 20 SECOND M_s

TABLE V-5

$M_s - m_b$ FIT SLOPE AND INTERCEPT VALUES

Period (sec)	Component	a	b	σ^2	Center of Mass		n
					m_b	M_s	
20	Vertical	1.72	-3.94	0.10	4.35	3.55	62
	Transverse	1.68	-3.61	0.11	4.33	3.66	66
	Radial	1.64	-3.59	0.09	4.32	3.50	64
30	Vertical	1.72	-4.15	0.10	4.34	3.30	61
	Transverse	1.59	-3.42	0.13	4.33	3.47	61
	Radial	1.71	-4.18	0.10	4.38	3.29	61
40	Vertical	1.51	-3.73	0.10	4.46	2.99	29
	Transverse	1.51	-3.57	0.09	4.40	3.09	36
	Radial	1.79	-4.98	0.11	4.42	2.92	24

where $M_s = am_b + b$

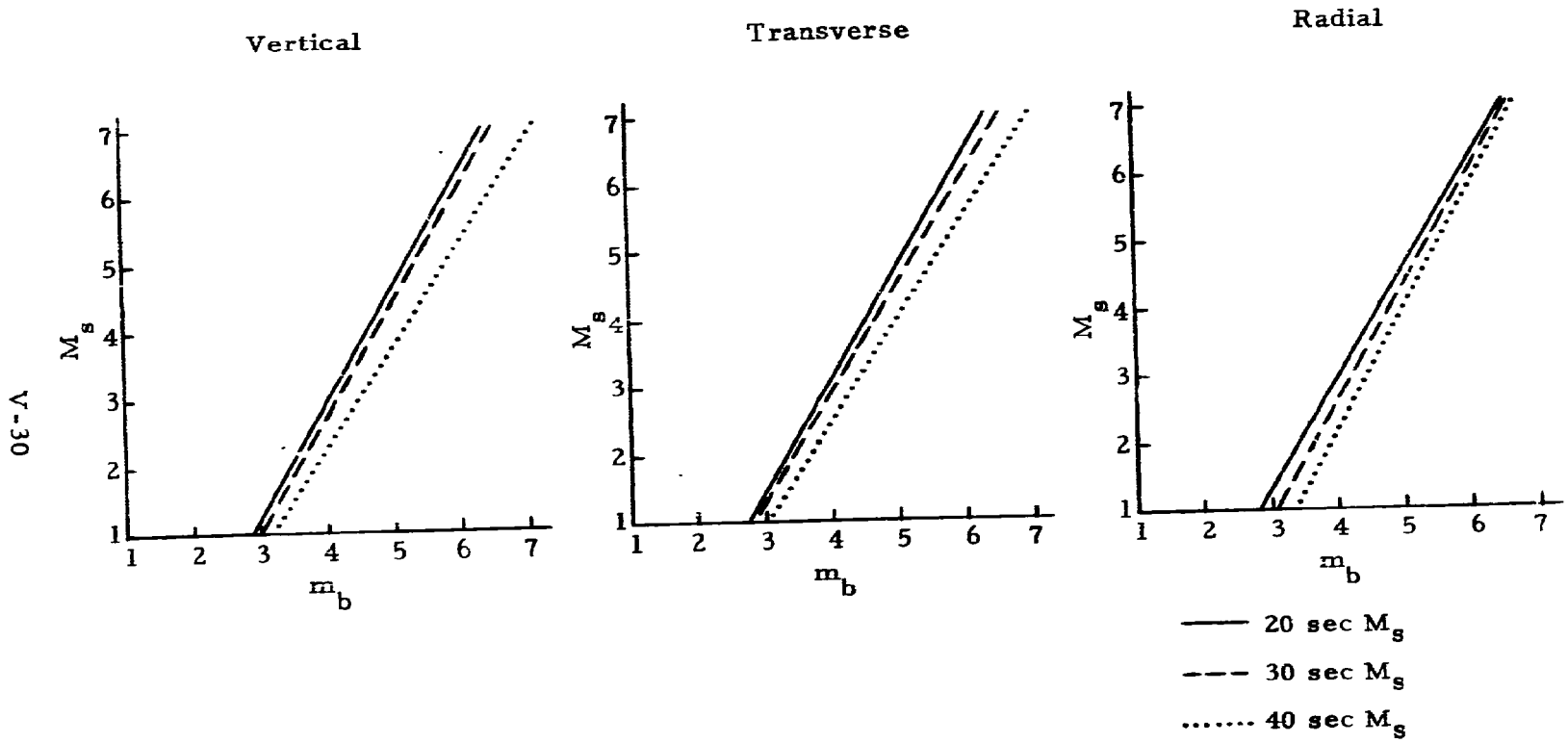

FIGURE V-16

M_s - m_b RELATIONSHIPS AT 20, 30, AND 40 SECONDS PERIOD

SECTION VI
CONCLUSIONS

In this section, we will summarize the results determined in this first evaluation of the Iranian Long Period Array. The major points are:

- The ILPA data quality is judged to be fairly good despite the various problems encountered in reading the data tapes. Of the 281 events in the data base, 84.0 percent were successfully processed, 1.8 percent were lost due to no data being recorded, 5.3 percent were lost to uncorrectable malfunctions, and 8.9 percent were lost to unreadable data.

- The highest gain in signal-to-noise ratio due to beamforming was 6.17 dB on the vertical component. Gains on the horizontal components averaged between 3 and 4 dB.

- The ILPA short-period 50 percent detection threshold was estimated to be 4.08 m_b units. Detection statistics used in making this estimation were obtained by visually reviewing develocorder films for events 1 to 45.

- The absolute 50 percent detection threshold for ILPA beam data is at $m_b = 4.55$ for Rayleigh waves and $m_b = 4.48$ for Love waves. Absolute detection thresholds were arrived at by counting all mixed events, events for which no data was available, events containing malfunctions, and events for which the data was unreadable as non-detections.

- The conditional 50 percent detection threshold for ILPA beam data is at $m_b = 4.09$ for Rayleigh waves and $m_b = 4.04$ for Love waves. Conditional detection thresholds were arrived at by including in the detection statistics only those events for which a detection/non-detection decision could be made.

- Beamforming lowered the conditional 50 percent detection threshold by approximately 0.15 m_b units.

- Indirect estimates of the 50 percent detection threshold made from noise samples agreed quite closely with the above described direct estimates.

- Combining the beam detection statistics of the individual components resulted in a conditional 50 percent detection threshold of $m_b = 4.01$ for the case where an event was declared detected if it was detected on one or more components. This conditional 50 percent detection threshold is $m_b = 4.13$ for the case where the event was declared detected only if it was detected on all three components.

- $M_s - m_b$ fits were computed at periods of 20, 30, and 40 seconds for earthquake data only, since the data base did not contain any presumed explosions. For this data base, the surface wave magnitude decreased with increasing period.

The major areas which must be investigated in the future to complete the evaluation of the Iranian Long Period Array are as follows:

- Noise analysis - A daily sampling of the noise field is needed to provide us with estimates of RMS noise levels, spectral content of the noise, and noise coherency.

- Signal analysis - The data base must be greatly expanded so that regional detection capability can be estimated. Also, the work on signal-to-noise ratio gains due to beamforming should be continued and expanded.

- Discrimination capability - Depth information for the earthquakes and a suite of presumed explosions must be obtained to determine the ILPA discrimination capability.

SECTION VII
REFERENCES

Ringdal, F., 1974, VLPE Network Evaluation and Automatic Processing Research, Technical Report No. 2, Texas Instruments Report No. ALEX(01)-TR-74-02, AFTAC Contract Number F08606-74-C-0033, Texas Instruments Incorporated, Dallas, Texas.

Unger, R., 1974, Estimating a Seismic Station's Detection Capability from Noise, Application to VLPE Stations, Technical Report No. 4, Texas Instruments Report No. ALEX(01)-TR-74-04, AFTAC Contract Number F08606-74-C-0033, Texas Instruments Incorporated, Dallas, Texas.

APPENDIX A

THE DATA BASE

In this appendix we present the parameters describing each of the events of the data base. The column headed "EVNO" gives the unique number assigned to each event. The column headed "DATE" gives the month, day, and year of occurrence of the event. The column headed "TIME" gives the event origin time. The columns headed "LAT" and "LONG" give the latitude and longitude of the event epicenter, where a positive value indicates north latitude or east longitude (as appropriate) and a negative value indicates south latitude or west longitude. The column headed "MB" gives the NORSAR value of the event bodywave magnitude. The column headed "LOCATION" gives the general seismic region in which the event occurred. Finally, the column headed "QUALITY" gives the NORSAR quality rating of the event parameters, where

1 = good to excellent

2 = fair to good

3 = poor to fair.

We note that all the event parameters listed were taken from the NORSAR event lists.

EVNO	DATE	TIME	LAT.	LONG.	MB	LOCATION	QUALITY
[illegible]	5/ 1/76	7.26.11	36.0	30.0	3.9	E. MEDITERRANEAN SEA	3
[illegible]	5/ 1/76	8.28.59	34.0	80.0	3.7	TIBET	3
[illegible]	5/ 1/76	11.35.33	38.0	89.0	4.1	S. SINKIANG PROV.	2
[illegible]	5/ 1/76	12.41.48	31.0	138.0	3.9	S. OF HONSHU, JAPAN	2
[illegible]	5/ 1/76	16.33.10	32.0	62.0	3.8	SW AFGHANISTAN	3
[illegible]	5/ 1/76	19.34.12	41.0	142.0	4.9	NEC HONSHU, JAPAN	1
[illegible]	5/ 2/76	0.25.29	35.0	27.0	3.5	CRETE	3
[illegible]	5/ 2/76	15.20.25	50.0	155.0	4.1	KURILE ISLANDS	2
[illegible]	5/ 2/76	15.29.54	37.0	139.0	4.3	NWC HONSHU, JAPAN	1
[illegible]	5/ 2/76	15.41.33	39.0	64.0	3.6	UZBEK SSR	3
[illegible]	5/ 2/76	16.37.30	53.0	158.0	3.7	NEC KAMCHATKA	3
[illegible]	5/ 2/76	16.57.26	30.0	51.0	4.1	IRAN	2
[illegible]	5/ 3/76	7.36.16	29.0	67.0	3.7	PAKISTAN	2
[illegible]	5/ 3/76	11. 3.29	40.0	76.0	3.7	KIRGIZ-SINKIANG BOR.	2
[illegible]	5/ 3/76	23.39.32	43.0	103.0	3.6	MONGOLIA	2
[illegible]	5/ 4/76	3.39.39	47.0	154.0	4.2	KURILE ISLANDS	1
[illegible]	5/ 4/76	5.23. 9	32.0	50.0	3.5	WESTERN IRAN	2
[illegible]	5/ 4/76	6. 1.51	29.0	98.0	4.3	TIBET	2
[illegible]	5/ 4/76	7. 5.11	27.0	81.0	3.5	NORTHERN INDIA	2
[illegible]	5/ 5/76	3.57. 6	37.0	69.0	4.4	AFGHAN.-USSR BORDER	2
[illegible]	5/ 5/76	12. 2.36	42.0	141.0	3.8	HOKKAIDO, JAPAN REG.	3
[illegible]	5/ 5/76	13.26.18	45.0	149.0	4.6	KURILE ISLANDS	1
[illegible]	5/ 5/76	16.13.22	44.0	146.0	3.5	HOKKAIDO, JAPAN REG.	3
[illegible]	5/ 5/76	17.54.33	37.0	73.0	3.7	AFGHAN.-USSR BORDER	2
[illegible]	5/ 5/76	1. 1.35	29.0	139.0	4.0	S. OF HONSHU, JAPAN	2
[illegible]	5/ 6/76	8.21.35	31.0	77.0	4.2	NORTHERN INDIA	2
[illegible]	5/ 6/76	11.13. 2	44.0	149.0	4.0	KURILE ISLANDS	2
[illegible]	5/ 6/76	16.53.26	43.0	80.0	4.2	KIRGIZ-SINKIANG BOR.	2
[illegible]	5/ 6/76	17.42.43	44.0	147.0	4.7	KURILE ISLANDS	1
[illegible]	5/ 6/76	17.59. 4	35.0	24.0	4.7	CRETE	2
[illegible]	5/ 6/76	19.59. 9	46.0	13.0	4.2	NORTHERN ITALY	2
[illegible]	5/ 6/76	20. 0.17	46.0	13.0	6.0	NORTHERN ITALY	2
[illegible]	5/ 6/76	20.25. 5	46.0	13.0	3.6	NORTHERN ITALY	2
[illegible]	5/ 6/76	20.36. 7	39.0	64.0	3.8	UZBEK SSR	2
[illegible]	5/ 6/76	21.42.25	46.0	13.0	3.7	NORTHERN ITALY	2
[illegible]	5/ 6/76	21.49.52	46.0	13.0	4.1	NORTHERN ITALY	2
[illegible]	5/ 7/76	0.10.42	39.0	64.0	4.5	UZBEK SSR	1
[illegible]	5/ 7/76	0.23.53	46.0	13.0	4.3	NORTHERN ITALY	3
[illegible]	5/ 7/76	1.33. 7	35.0	72.0	4.2	PAKISTAN	2
[illegible]	5/ 7/76	2. 9.54	43.0	140.0	4.0	HOKKAIDO, JAPAN REG.	2

TABLE A-1

EVENT PARAMETERS
(PAGE 1 OF 7)

EVNO	DATE	TIME	LAT.	LONG.	MB	LOCATION	QUALITY
[illegible]	5/ 7/76	4.34.20	48.0	154.0	3.9	KURILE ISLANDS	2
[illegible]	5/ 7/76	13.44.25	46.0	13.0	3.2	NORTHERN ITALY	3
[illegible]	5/ 7/76	18. 2.53	32.0	78.0	3.8	KASHMIR-TIBET BOR.	3
[illegible]	5/ 7/76	23. 5.23	40.0	29.0	3.6	TURKEY	3
[illegible]	5/ 8/76	3.10.17	46.0	13.0	3.9	NORTHERN ITALY	2
[illegible]	5/ 8/76	16.36.38	34.0	135.0	3.7	NSC HONSHU, JAPAN	3
[illegible]	5/ 8/76	19.39.59	31.0	131.0	3.8	KYUSHU, JAPAN	2
[illegible]	5/ 9/76	0.53.49	46.0	13.0	5.1	NORTHERN ITALY	2
[illegible]	5/ 9/76	2.55.58	40.0	30.0	3.8	TURKEY	3
[illegible]	5/ 9/76	5.53.45	36.0	22.0	3.6	MEDITERRANEAN SEA	3
[illegible]	5/ 9/76	7.51.25	41.0	63.0	5.0	UZBEK SSR	2
[illegible]	5/ 9/76	8.13. 4	45.0	149.0	3.5	KURILE ISLANDS	3
[illegible]	5/ 9/76	10. 7.12	37.0	66.0	3.6	AFGHAN.-USSR BORDER	3
[illegible]	5/ 9/76	11.19.47	40.0	30.0	4.0	TURKEY	3
[illegible]	5/ 9/76	13.21.16	46.0	13.0	2.9	AUSTRIA	3
[illegible]	5/ 9/76	13.14.27	35.0	140.0	4.2	NEC HONSHU, JAPAN	2
[illegible]	5/ 9/76	15. 1.25	40.0	30.0	4.1	TURKEY	2
[illegible]	5/ 9/76	16.30.25	46.0	150.0	3.6	KURILE ISLANDS	2
[illegible]	5/ 9/76	21.11. 8	40.0	30.0	3.3	TURKEY	3
[illegible]	5/ 9/76	22. 5.17	46.0	35.0	2.6	CRIMEA REGION	3
[illegible]	5/10/76	3. 2.20	35.0	72.0	3.4	PAKISTAN	3
[illegible]	5/10/76	5.24.54	40.0	73.0	3.7	TADZHIK-SINKIANG BOR	2
[illegible]	5/10/76	8.34.31	39.0	19.0	3.5	GREECE-ALBANIA BOR.	3
[illegible]	5/10/76	9.43.47	31.0	141.0	3.7	S. OF HONSHU, JAPAN	3
[illegible]	5/10/76	8.14.56	39.0	15.0	3.3	SICILY	2
[illegible]	5/10/76	12. 1.38	40.0	29.0	4.2	TURKEY	3
[illegible]	5/10/76	15.20.49	39.0	30.0	4.2	TURKEY	2
[illegible]	5/10/76	18.37.28	29.0	82.0	4.0	NEPAL	3
[illegible]	5/10/76	18.43.40	28.0	83.0	5.0	NEPAL-INDIA BOR.	2
[illegible]	5/10/76	23.34.15	46.0	36.0	2.8	SOUTHWESTERN RUSSIA	3
[illegible]	5/11/76	23.54.14	40.0	30.0	4.3	TURKEY	2
[illegible]	5/11/76	3. 2. 3	30.0	81.0	3.4	NEPAL	3
[illegible]	5/11/76	3.32. 8	40.0	30.0	4.2	TURKEY	3
[illegible]	5/11/76	5. 4.16	36.0	141.0	4.1	NEC HONSHU, JAPAN	2
[illegible]	5/11/76	7.14.13	33.0	53.0	3.8	IRAN	3
[illegible]	5/11/76	11.48.33	36.0	71.0	3.6	PAKISTAN	2
[illegible]	5/11/76	13.26.51	45.0	149.0	4.2	KURILE ISLANDS	2
[illegible]	5/11/76	17. 3.23	41.0	21.0	5.5	GREECE-ALBANIA BOR.	2
[illegible]	5/11/76	17. 9.55	36.0	22.0	5.2	MEDITERRANEAN SEA	2
[illegible]	5/11/76	19.25. 0	32.0	49.0	3.4	WESTERN IRAN	3

TABLE A-1

EVENT PARAMETERS
(PAGE 2 OF 7)

EVNO	DATE	TIME	LAT.	LONG.	MB	LOCATION	QUALITY
[illegible]	5/11/76	21.11.51	36.0	22.0	4.[illegible]	MEDITERRANEAN SEA	3
[illegible]	5/11/76	22.44. [illegible]	46.0	14.0	5.0	NORTHERN ITALY	2
[illegible]	5/12/76	[illegible]5.11.49	40.0	30.0	4.1	TURKEY	2
[illegible]	5/12/76	5.26.16	38.0	21.0	3.2	IONIAN SEA	3
[illegible]	5/12/76	7.43.54	36.0	71.0	4.3	AFGHAN-USSR BORDER	2
[illegible]	5/12/76	16.23.17	34.0	72.0	4.0	PAKISTAN	2
[illegible]	5/12/76	16.45.40	52.0	160.0	4.1	OEC KAMCHATKA	2
[illegible]	5/12/76	18. 5.20	38.0	21.0	2.9	IONIAN SEA	3
[illegible]	5/12/76	18.40.15	42.0	146.0	4.4	OC HOKKAIDO, JAPAN	2
[illegible]	5/13/76	[illegible].44.48	43.0	20.0	4.0	YUGOSLAVIA	2
[illegible]	5/13/76	9.5[illegible].1[illegible]	44.0	149.0	3.9	KURILE ISLANDS	2
[illegible]	5/13/76	11. [illegible]. 8	36.0	140.0	3.8	HONSHU, JAPAN	3
[illegible]	5/13/76	13. 5. 2	46.0	12.0	4.0	NORTHERN ITALY	2
[illegible]	5/13/76	13.18.29	40.0	30.0	3.6	TURKEY	3
[illegible]	5/13/76	14.47.34	36.0	22.0	3.5	MEDITERRANEAN SEA	3
[illegible]	5/13/76	19.23. 1	38.0	21.0	2.8	IONIAN SEA	3
[illegible]	5/13/76	20.28.46	35.0	140.0	4.5	NEC HONSHU, JAPAN	2
[illegible]	5/13/76	20.44.32	35.0	24.0	4.2	CRETE	2
[illegible]	5/13/76	21.13. 5	38.0	21.0	3.1	IONIAN SEA	3
[illegible]	5/13/76	22.17.48	36.0	22.0	4.0	MEDITERRANEAN SEA	2
[illegible]	5/13/76	23.17.21	40.0	143.0	3.8	NEC HONSHU, JAPAN	2
[illegible]	5/14/76	1.23.17	38.0	32.0	3.5	TURKEY	3
[illegible]	5/14/76	11. 6.17	39.0	30.0	3.9	TURKEY	3
[illegible]	5/14/76	11.56.22	35.0	72.0	3.9	PAKISTAN	2
[illegible]	5/14/76	16. 1.30	43.0	149.0	4.2	KURILE ISLANDS REG.	2
[illegible]	5/14/76	18.51.48	49.0	150.0	3.6	NW OF KURILE ISLANDS	3
[illegible]	5/14/76	20.24.53	39.0	142.0	3.9	NEC HONSHU, JAPAN	3
[illegible]	5/14/76	20.40.13	41.0	144.0	5.2	HOKKAIDO, JAPAN	1
[illegible]	5/14/76	22.27.54	40.0	143.0	3.9	NEC HONSHU, JAPAN	2
[illegible]	5/15/76	3. 3.25	35.0	24.0	4.2	CRETE	2
[illegible]	5/15/76	4.24. 3	35.0	27.0	3.5	CRETE	3
[illegible]	5/15/76	4.35.11	41.0	69.0	3.4	TADZHIK SSR	2
[illegible]	5/15/76	6.55.54	24.0	94.0	3.5	BURMA-INDIA BOR.	3
[illegible]	5/15/76	8.11.59	19.0	95.0	4.8	BURMA	1
[illegible]	5/15/76	11. 6. 6	40.0	30.0	3.4	TURKEY	2
[illegible]	5/15/76	19.12.28	38.0	21.0	2.8	IONIAN SEA	3
[illegible]	5/15/76	22.23.29	42.0	141.0	3.7	HOKKAIDO, JAPAN REG.	3
[illegible]	5/15/76	23. 6.23	38.0	144.0	3.8	OEC HONSHU, JAPAN	3
[illegible]	5/16/76	8. 1.16	36.0	51.0	3.7	IRAN	2
[illegible]	5/16/76	13.59. 8	35.0	72.0	3.8	PAKISTAN	2

TABLE A-1

EVENT PARAMETERS
(PAGE 3 OF 7)

EVNO	DATE	TIME	LAT.	LONG.	MB	LOCATION	QUALITY
0121	5/16/76	15.48.36	36.0	74.0	3.5	NORTHWESTERN KASHMIR	3
0122	5/16/76	20.25.16	48.0	154.0	4.2	KURILE ISLANDS	2
0123	5/17/76	2.58.35	39.0	64.0	6.5	UZBEK SSR	1
0124	5/17/76	3.21.39	39.0	64.0	4.3	UZBEK SSR	2
0125	5/17/76	3.29.14	39.0	64.0	4.1	UZBEK SSR	2
0126	5/17/76	3.57.25	41.0	62.0	4.1	TURKMEN SSR	2
0127	5/17/76	4.14.26	42.0	62.0	4.4	UZBEK SSR	2
0128	5/17/76	4.34.33	39.0	65.0	3.5	TURKMEN SSR	2
0129	5/17/76	4.54.15	42.0	61.0	4.7	TURKMEN SSR	2
0130	5/17/76	5.53.10	39.0	64.0	4.0	UZBEK SSR	2
0131	5/17/76	6. 6.32	39.0	64.0	3.2	TURKMEN SSR	3
0132	5/17/76	6.37. 8	41.0	61.0	3.8	UZBEK SSR	2
0133	5/17/76	6.58.11	39.0	64.0	3.8	UZBEK SSR	2
0134	5/17/76	7.20. 3	41.0	63.0	3.6	UZBEK SSR	3
0135	5/17/76	8.10.26	39.0	64.0	3.8	TURKMEN SSR	2
0136	5/17/76	10.44.12	41.0	63.0	3.4	UZBEK SSR	2
0137	5/17/76	11. 1.36	41.0	62.0	4.0	UZBEK SSR	2
0138	5/17/76	15.39.16	40.0	30.0	3.7	TURKEY	3
0139	5/17/76	16.11.36	38.0	21.0	3.7	IONIAN SEA	3
0140	5/17/76	16.38.10	41.0	63.0	3.2	UZBEK SSR	3
0141	5/17/76	17.46.18	40.0	64.0	4.7	UZBEK SSR	2
0142	5/17/76	20.18.24	42.0	62.0	3.5	UZBEK SSR	3
0143	5/17/76	21.52.28	41.0	62.0	3.7	UZBEK SSR	2
0144	5/17/76	22.18.25	56.0	162.0	4.8	NEC KAMCHATKA	1
0145	5/18/76	2.17.45	31.0	130.0	3.9	KYUSHU, JAPAN	3
0146	5/18/76	5.35.37	43.0	61.0	3.4	UZBEK SSR	3
0147	5/18/76	6.16.43	44.0	82.0	3.6	N. SINKIANG PROV.	2
0148	5/18/76	7.59.41	35.0	27.0	3.3	CRETE	3
0149	5/18/76	8.30.14	35.0	27.0	4.2	CRETE	3
0150	5/18/76	8.57.37	41.0	63.0	4.6	UZBEK SSR	1
0151	5/18/76	13.54.33	41.0	62.0	4.8	TURKMEN SSR	1
0152	5/18/76	14.30. 9	32.0	130.0	4.5	KYUSHU, JAPAN	1
0153	5/18/76	15. 5.28	31.0	130.0	3.8	KYUSHU, JAPAN	2
0154	5/18/76	16. 1.39	31.0	130.0	4.1	KYUSHU, JAPAN	2
0155	5/18/76	16.15.50	38.0	21.0	3.5	IONIAN SEA	3
0156	5/18/76	17. 7.51	38.0	21.0	2.8	IONIAN SEA	3
0157	5/18/76	17.15.28	50.0	152.0	3.9	NW OF KURILE IS.	3
0158	5/18/76	20.11.39	39.0	64.0	3.7	TURKMEN SSR	2
0159	5/18/76	20.22. 2	39.0	64.0	3.6	UZBEK SSR	2
0160	5/18/76	20.24.29	39.0	145.0	3.6	OEC HONSHU, JAPAN	3

TABLE A-1

EVENT PARAMETERS
(PAGE 4 OF 7)

EVNO	DATE	TIME	LAT.	LONG.	MB	LOCATION	QUALITY
0161	5/18/76	21.31.34	31.0	130.0	3.5	KYUSHU, JAPAN	3
0162	5/18/76	22. 0.44	35.0	71.0	3.5	PAKISTAN	2
0163	5/18/76	22.48.47	39.0	64.0	3.4	TURKMEN SSR	2
0164	5/18/76	23. 9.47	36.0	22.0	3.5	MEDITERRANEAN SEA	3
0165	5/19/76	1.11.12	39.0	64.0	4.2	UZBEK SSR	1
0166	5/19/76	2.26. 9	41.0	63.0	3.5	UZBEK SSR	3
0167	5/19/76	2.56.48	49.0	80.0	4.6	EASTERN KAZAKH SSR	1
0168	5/19/76	7.30.16	39.0	65.0	3.6	TURKMEN SSR	3
0169	5/19/76	10. 8.21	48.0	112.0	4.0	MONGOLIA	2
0170	5/19/76	15.54.54	41.0	62.0	4.8	TURKMEN SSR	1
0171	5/19/76	16.44. 9	38.0	21.0	3.0	IONIAN SEA	3
0172	5/20/76	1. 2.13	42.0	71.0	3.7	KIRGIZ SSR	3
0173	5/20/76	2.57. 3	39.0	65.0	3.8	SE UZBEK SSR	2
0174	5/20/76	6.43.33	33.0	55.0	3.9	IRAN	2
0175	5/20/76	11.28. 6	36.0	73.0	3.9	AFGHAN.-USSR BORDER	2
0176	5/20/76	11.37.15	39.0	64.0	3.9	UZBEK SSR	2
0177	5/20/76	12. 1.33	56.0	44.0	2.7	WESTERN RUSSIA	3
0178	5/20/76	12.50.26	38.0	70.0	3.5	AFGHAN.-USSR BORDER	3
0179	5/20/76	17. 0.22	30.0	128.0	4.6	EAST CHINA SEA	1
0180	5/20/76	19.42.43	46.0	152.0	4.3	KURILE ISLANDS	2
0181	5/20/76	22. 4.24	45.0	149.0	3.8	KURILE ISLANDS	2
0182	5/21/76	0.11.49	35.0	72.0	3.7	PAKISTAN	2
0183	5/21/76	0.50.41	51.0	155.0	3.7	KURILE ISLANDS	3
0184	5/21/76	4.33.36	41.0	63.0	3.4	UZBEK SSR	3
0185	5/21/76	12. 6.26	33.0	74.0	3.8	SOUTHWEST KASHMIR	3
0186	5/21/76	13. 0.18	37.0	140.0	3.6	HONSHU, JAPAN	3
0187	5/21/76	16. 5.21	39.0	64.0	4.2	UZBEK SSR	1
0188	5/21/76	16.25.54	30.0	142.0	4.5	SOUTH OF HONSHU	1
0189	5/21/76	18.28.50	39.0	64.0	3.9	UZBEK SSR	2
0190	5/22/76	18. 2. 8	40.0	29.0	3.9	TURKEY	3
0191	5/22/76	18.32.36	31.0	76.0	3.8	NORTHERN INDIA	2
0192	5/22/76	18.51.11	46.0	148.0	3.8	KURILE ISLANDS	2
0193	5/23/76	3.53.58	39.0	30.0	3.6	TURKEY	3
0194	5/23/76	9.20.52	38.0	21.0	2.8	IONIAN SEA	3
0195	5/23/76	9.49.19	39.0	64.0	4.0	UZBEK SSR	2
0196	5/23/76	10.58.33	40.0	143.0	4.1	NEC HONSHU, JAPAN	2
0197	5/23/76	13.26.48	39.0	64.0	3.4	UZBEK SSR	2
0198	5/24/76	6.10.46	39.0	64.0	3.8	UZBEK SSR	2
0199	5/24/76	6.49.44	47.0	152.0	3.8	KURILE ISLANDS	3
0200	5/24/76	9.36.49	51.0	59.0	2.8	WESTERN KAZAKH SSR	3

TABLE A-1

EVENT PARAMETERS
(PAGE 5 OF 7)

EVNO	DATE	TIME	LAT.	LONG.	MB	LOCATION	QUALITY
[illegible]	5/24/76	11.24.26	32.0	142.0	5.4	SOUTH OF HONSHU	1
[illegible]	5/24/76	14.56.25	41.0	62.[illegible]	4.3	UZBEK SSR	2
[illegible]	5/24/76	17.52. 7	44.[illegible]	12.[illegible]	3.7	CENTRAL ITALY	3
[illegible]	5/25/76	[illegible].12.22	33.[illegible]	141.0	3.7	SOUTH OF HONSHU	3
[illegible]	5/25/76	2.22.19	43.[illegible]	136.0	3.3	E. SEA OF JAPAN	3
[illegible]	5/25/76	4.48.49	27.0	94.0	4.6	EASTERN INDIA	1
[illegible]	5/25/76	7.29.11	44.[illegible]	148.0	3.6	KURILE ISLANDS	3
[illegible]	5/25/76	8. 9.17	53.[illegible]	158.0	5.5	NEC KAMCHATKA	1
[illegible]	5/25/76	8.16.53	53.[illegible]	158.0	5.7	NEC KAMCHATKA	1
[illegible]	5/25/76	[illegible].53.16	53.[illegible]	158.[illegible]	4.0	NEC KAMCHATKA	2
[illegible]	5/25/76	11. 9.42	56.[illegible]	158.0	4.6	KURILE ISLANDS	2
[illegible]	5/25/76	11.17. 3	52.[illegible]	160.[illegible]	3.9	OEC KAMCHATKA	2
[illegible]	5/25/76	12.12.42	32.[illegible]	50.0	3.4	WESTERN IRAN	3
[illegible]	5/25/76	15.34.2[illegible]	51.[illegible]	158.[illegible]	4.1	KURILE ISLANDS	2
[illegible]	5/25/76	18.43.25	39.[illegible]	30.0	4.6	TURKEY	2
[illegible]	5/25/76	23.33.39	31.[illegible]	143.[illegible]	4.6	SOUTH OF HONSHU	1
[illegible]	5/26/76	2.15. [illegible]	40.[illegible]	73.0	3.5	KIRGIZ SSR	3
[illegible]	5/26/76	17.2[illegible].22	23.[illegible]	120.[illegible]	4.0	TAIWAN REGION	3
[illegible]	5/27/76	2.19.49	31.[illegible]	83.[illegible]	3.6	TIBET	3
[illegible]	5/27/76	4.24.51	36.[illegible]	68.0	3.8	HINDU KUSH REGION	3
[illegible]	5/27/76	6.44.14	40.[illegible]	64.0	3.7	UZBEK SSR	2
[illegible]	5/27/76	[illegible].16.49	30.[illegible]	142.0	3.9	SOUTH OF HONSHU	3
[illegible]	5/27/76	17.[illegible]. 6	37.[illegible]	70.0	3.8	HINDU KUSH REGION	3
[illegible]	5/28/76	3.36.43	36.[illegible]	139.[illegible]	3.9	HONSHU, JAPAN	2
[illegible]	5/28/76	4.52.49	55.[illegible]	109.0	3.9	LAKE BAIKAL REGION	2
[illegible]	5/28/76	14. 5.31	39.[illegible]	64.[illegible]	4.8	UZBEK SSR	1
[illegible]	5/28/76	15.51.35	52.[illegible]	51.0	3.2	WESTERN KAZAKH SSR	3
[illegible]	5/28/76	23. 2.19	39.[illegible]	30.0	4.4	TURKEY	2
[illegible]	5/28/76	23. 9.54	43.[illegible]	35.0	3.2	BLACK SEA	3
[illegible]	5/29/76	1.59. 9	35.0	140.[illegible]	3.7	NEC HONSHU, JAPAN	3
[illegible]	5/29/76	3.45.33	39.[illegible]	30.0	3.9	TURKEY	2
[illegible]	5/29/76	4.45.48	25.[illegible]	123.[illegible]	4.3	SW RYUKYU ISLANDS	1
[illegible]	5/29/76	8.38.22	39.[illegible]	114.[illegible]	3.7	NORTHEASTERN CHINA	3
[illegible]	5/29/76	[illegible].21.13	38.[illegible]	21.0	2.8	IONIAN SEA	3
[illegible]	5/29/76	11.42.47	56.0	162.0	3.7	NEC KAMCHATKA	3
[illegible]	5/29/76	11.58.39	27.0	97.0	4.7	BURMA	1
[illegible]	5/29/76	12.23.13	24.0	100.0	5.7	BURMA-CHINA BORDER	1
[illegible]	5/29/76	12.35.36	28.0	96.0	4.2	INDIA-CHINA BORDER	2
[illegible]	5/29/76	12.59. 5	25.0	97.0	3.8	BURMA-CHINA BORDER	3
[illegible]	5/29/76	13.55.51	28.0	96.0	4.0	INDIA-CHINA BORDER	3

TABLE A-1

EVENT PARAMETERS
(PAGE 6 OF 7)

EVNO	DATE	TIME	LAT.	LONG.	MB	LOCATION	QUALITY
0241	5/29/76	14. 7.16	28.0	99.0	6.2	BURMA-CHINA BORDER	1
0243	5/29/76	14.11.14	28.0	96.0	3.8	INDIA-CHINA BORDER	3
0243	5/29/76	14.28.32	28.0	96.0	3.7	INDIA-CHINA BORDER	3
0244	5/29/76	14.32. 7	27.0	97.0	4.7	BURMA	2
0245	5/29/76	14.53.10	26.0	98.0	4.4	BURMA-CHINA BORDER	2
0246	5/29/76	15. 3. 9	28.0	95.0	3.7	INDIA-CHINA BORDER	3
0247	5/29/76	15.26.15	40.0	30.0	3.4	TURKEY	3
0248	5/29/76	16. 5.44	24.0	98.0	3.8	BURMA-CHINA BORDER	3
0249	5/29/76	17. 9.15	27.0	97.0	3.8	BURMA	3
0250	5/29/76	18.25.53	31.0	77.0	3.2	NORTHERN INDIA	3
0251	5/29/76	19.37.25	28.0	96.0	5.1	INDIA-CHINA BORDER	2
0252	5/29/76	21.57.13	41.0	20.0	3.2	GREECE-ALBANIA BOR.	3
0253	5/29/76	22. 5.19	35.0	24.0	3.5	CRETE	2
0254	5/29/76	23.12.11	37.0	140.0	4.3	HONSHU, JAPAN	2
0255	5/29/76	23.31.29	25.0	99.0	3.8	YUNNAN PROV. CHINA	3
0256	5/30/76	0.40.12	28.0	99.0	3.9	BURMA-CHINA BORDER	3
0257	5/30/76	2.26. 6	39.0	73.0	3.8	TADZHIK-SINKIANG BOR	2
0258	5/30/76	3.15.19	39.0	64.0	3.4	UZBEK SSR	3
0259	5/30/76	4. 2.28	34.0	72.0	4.0	PAKISTAN	2
0260	5/30/76	4.19. 4	27.0	97.0	4.9	BURMA	2
0261	5/30/76	4.53.52	43.0	17.0	3.1	ADRIATIC SEA	3
0262	5/30/76	5.32.34	34.0	47.0	3.7	WESTERN IRAN	2
0263	5/30/76	8. 1.48	52.0	160.0	4.0	OFC KAMCHATKA	1
0264	5/30/76	13.11.47	53.0	157.0	4.3	KAMCHATKA	1
0265	5/30/76	13.16.29	31.0	143.0	4.0	SOUTH OF HONSHU	2
0266	5/30/76	13.46.11	41.0	21.0	3.3	GREECE-ALBANIA BOR.	2
0267	5/30/76	16.27.21	41.0	21.0	3.2	GREECE-ALBANIA BOR.	2
0268	5/30/76	17.31.18	34.0	48.0	3.3	WESTERN IRAN	3
0269	5/30/76	19.43.39	25.0	97.0	3.7	BURMA-CHINA BORDER	3
0270	5/30/76	21.12.43	43.0	13.0	3.2	CENTRAL ITALY	3
0271	5/30/76	21.47.33	27.0	128.0	4.3	RYUKYU ISLANDS	1
0272	5/30/76	22.16.29	41.0	77.0	3.8	KIRGIZ-SINKIANG BOR.	3
0273	5/30/76	22.31.31	24.0	98.0	4.4	BURMA-CHINA BORDER	1
0274	5/31/76	4.57.10	36.0	51.0	3.9	IRAN	3
0275	5/31/76	5. 8.35	25.0	99.0	5.3	YUNNAN PROV. CHINA	1
0276	5/31/76	8. 6. 7	32.0	61.0	4.6	IRAN	2
0277	5/31/76	13.17.19	47.0	154.0	4.6	KURILE ISLANDS	1
0278	5/31/76	18.35.35	28.0	96.0	5.1	INDIA-CHINA BORDER	2
0279	5/31/76	20.31.48	38.0	21.0	3.1	IONIAN SEA	3
0280	5/31/76	20.51.38	43.0	150.0	3.6	KURILE ISLANDS REG.	3
0281	5/31/76	20.56.53	31.0	130.0	4.1	KYUSHU, JAPAN	3

TABLE A-1

EVENT PARAMETERS
(PAGE 7 OF 7)